Fullerene–porphyrin architectures; photosynthetic antenna and reaction center models

Dirk M. Guldi

Radiation Laboratory, University of Notre Dame, IN 46556, USA. E-mail: guldi.1@nd.edu

Received 31st July 2001
First published as an Advance Article on the web 13th December 2001

Fullerenes and porphyrins are molecular architectures ideally suited for devising integrated, multicomponent model systems to transmit and process solar energy. Implementation of C_{60} as a 3-dimensional electron acceptor holds great expectations on account of their small reorganization energy in electron transfer reactions and has exerted a noteworthy impact on the improvement of light-induced charge-separation. This article describes how the specific compositions of porphyrin chromophores linked to C_{60}—yielding artificial light harvesting antenna and reaction center mimics—have been elegantly utilized to tune the electronic couplings between donor and acceptor sites and the total reorganization energy. Specifically, the effects that these parameters have on the rate, yield and lifetime of the energetic charge-separated states are considered.

1 Introduction

In photosynthesis, cascades of short-range energy transfer and electron transfer events occur between well-arranged organic pigments (*i.e.*, light harvesting antenna ensemble and photosynthetic reaction center (PRC)) and other cofactors.[1] Thereby the antenna portion captures light and transduces the resulting excitation energy, *via* singlet–singlet energy transfer, to the PRC. In the PRC charges are then separated with remarkable efficiency to yield a spatially and electronically well-isolated radical pair. Key to this success is, without any doubt, the overall small reorganization energy ($\lambda \sim 0.2$ eV) exhibited by the PRC and the well-balanced electronic coupling between each donor and acceptor. The arrangement of the donor–acceptor couples in the PRC is simple and accomplished *via* their non-covalent incorporation into well-defined transmembrane proteins. Owing to the importance and complexity of natural photosynthesis, the study thereof necessitates suitable simpler models. The ultimate goal is to design and assemble artificial systems, which can efficiently process solar energy, replicating the natural analog.[2]

Dirk M. Guldi graduated from the University of Cologne (Germany) in 1988, from where he received his PhD in 1990. In 1992, after a postdoctoral appointment at the National Institute of Standards and Technology, he took a research position at the Hahn-Meitner-Institute Berlin. After a brief stay as a Feodor-Lynen Stipend (Alexander von Humboldt Foundation) at Syracuse University he joined in 1995 the faculty of the Notre Dame Radiation Laboratory where he was promoted to Associate Scientist in 1996. In 1999 he completed his Habilitation at the University of Leipzig (Germany). He was awarded the 'Heisenberg-Prize' (1999; Deutsche Forschungsgemeinschaft) and 'Grammaticakis-Neumann-Prize' (2000; Swiss Society for Photochemistry and Photophysics). His primary research interests are in the areas of charge separation in super- and supramolecular systems with three-dimensional electron acceptors and organized thin films at semiconductor surfaces as tools viable for the efficient conversion of solar energy.

The rich and extensive absorptions (*i.e.*, π–π^* transitions) seen in porphyrinoid systems—the pigments of life—hold particular promise for increased absorptive cross sections and, thus, an efficient use of the solar spectrum. Over the course of recent years they emanate as light harvesting building blocks in the construction of molecular architectures.[3] Their high electronic excitation energy, typically exceeding 2.0 eV, powers a strongly exergonic electron transfer, which subsequently intercedes the conversion between light and chemical/electrical energy.

The search for an electron transfer partner brings us, however, well beyond components found in photosynthesis on earth, namely, $\mathbf{C_{60}}$. In fact, its discovery was attained in conjunction with compositionary issues in the interstellar medium.[4] This new three-dimensional electron acceptor is now readily available and exhibits exciting characteristics. The delocalization of charges—electrons or holes—within the giant, spherical carbon framework (diameter > 7.5 Å) together with the rigid, confined structure of the aromatic π-sphere offers unique opportunities for stabilizing charged entities. Six equally-spaced reduction waves in electrochemical experiments,[5] with the first reduction step resembling that of quinones—the electron acceptor unit in PRC proteins which is reduced to a semiquinone and finally to a hydroquinone—are a first manifestation of conditions that guarantee the optimal delocalization of charges. In other words, even in a highly reduced fullerene state (*i.e.*, tetraanion, pentaanion and hexaanion) electrons, as they are subsequently added to the fullerene's π-system, experience little, if any, repulsive forces. From this observation we infer the potential of fullerenes to possess quite small reorganization energies in electron transfer reactions, which renders application of this carbon material as electron accepting moieties particularly appealing under aspects of energy conversion and energy storage.

Thanks to the pioneering protocols, regarding the general chemical functionalization of fullerenes,[6] virtually any functional group can be covalently linked with any specific regioisomeric pattern to the highly reactive carbon framework *en route* to synthetic models of light harvesting arrays and reaction centers.

DOI: 10.1039/b106962b

2 Reorganization energy of fullerenes in electron transfer reactions

The total reorganization energy (λ) is composed of a solvent-independent and a solvent-dependent fragment, λ_v and λ_s, respectively.[7] In $\mathbf{C_{60}}$, the λ_v contribution, stemming from different nuclear configurations associated with the transformation, for instance, in a photochemical reaction from an initial to a final state, is very small ($\lambda_v \sim 0.06$ eV).[8] A sound interpretation for this striking observation implies the structural similarity between $\mathbf{C_{60}}$ in the ground, reduced and also excited state. This relates primarily to the rigidity of these spherical carbon structures (*i.e.*, high strain energy), preventing major structural or geometrical changes at room temperature. Further support for this conclusion was lent from small Stokes shifts in excitation experiments and small Raman shifts under reductive conditions. It is also believed that the solvent-dependent term is small, thus requiring only little energy for the adjustment of a generated state (*e.g.*, excited or reduced state) to the new solvent environment. This corresponds directly to the symmetrical shape and large size of the fullerene framework.

The sum of these effects bears fundamental consequences upon the classical Marcus treatment of electron transfer reactions. In particular, the Marcus theory predicts that the dependence of electron transfer rates on the free energy changes of the reaction ($-\Delta G_{ET}°$) is a parabolic curve.[7] In the 'normal region' of the Marcus curve ($-\Delta G_{ET}° < \lambda$) the theory predicts an increase in rate with increasing thermodynamic driving force until optimal conditions are reached, when the driving force equals the overall reorganization energy ($-\Delta G_{ET}° \sim \lambda$). Beyond this thermodynamic maximum the highly exergonic region ($-\Delta G_{ET}° > \lambda$) is entered, where the rate constants start to decrease with increasing free energy changes ('inverted region'). Variation of λ is not only the key to control the maximum of the parabola, but, most importantly, to influence the shape of the underlying dependence. In principle, smaller λ-values assist in reaching the maximum of the Marcus parabola at smaller $-\Delta G_{ET}°$ values and, in turn, in shifting the energy-wasting charge-recombination deep into the Marcus 'inverted region'.

Our own studies, focusing on pulse-radiolytic electron transfer dynamics between fullerenes and a series of radiolytically generated arene π-radical cations, $(\mathbf{arene})^{\cdot+}$, with varying oxidation potentials were designed to efficaciously exploit their reorganization energy.[9] Interestingly, parabolic dependencies of the rate constants on the thermodynamic driving force ($-\Delta G_{ET}°$) were found for *inter*molecular reactions involving the higher fullerenes $\mathbf{C_{76}}$ and $\mathbf{C_{78}}$. It should be noted that these cases represent some of the rare confirmations of the existence of the 'inverted region' in a truly *inter*molecular forward electron transfer. From these experiments an experimental value of *ca.* 0.6 eV (in dichloromethane) was deduced for the total reorganization energy (λ) of $\mathbf{C_{76}}$ and $\mathbf{C_{78}}$ in oxidative electron transfer processes. A more recent follow-up work, in which the electrochemically determined oxidation potentials are used for the ($-\Delta G_{ET}°$) *versus* (k_{ET}) dependence, instead of the ionization potentials, suggests an even smaller value.

$$C_{76}/C_{78} + (\text{arene})^{\cdot+} \rightarrow (C_{76})^{\cdot+}/(C_{78})^{\cdot+} + \text{arene}$$

3 Porphyrin–fullerene van der Waals interactions

Another fascinating scenario involves the utilization of strong π–π associations between metalloporphyrins (**MP**), in general, and fullerenes as a means to engineer supramolecular arrays with remarkable photoactive and magnetic properties.[10] This aspect was systematically explored in a series of $\mathbf{MP/C_{60}}$ cocrystallates with **M** being Mn, Co, Ni, Cu, Zn and Fe. Favorable van der Waals attractions between the curved π-surface of the fullerene and the planar π-surface of **MP**, assist in the supramolecular recognition, overcoming, however, the necessity of matching a concave-shaped host with a convex-shaped guest structure. This leads to complexes with unusually short contacts (2.7–3.0 Å), shorter than ordinary van der Waals contacts (3.0–3.5 Å), and a variety of crystal structures, ranging from zigzag-chains to columns (Fig. 1).

In conclusion, van der Waals attractions between porphyrins and fullerenes, which are also appreciable in condensed media (*vide infra*), constitute an important organization principle: whenever affirmed by the molecular topology of the system these moieties spontaneously tend to achieve close spatial proximity relative to each other.

4 *Inter*molecular electron transfer reactions

The first $\mathbf{ZnP/C_{60}}$ system probed was part of a larger investigation, focusing on *inter*molecular electron transfer reactions between a series of radiolytically generated one-electron reduced metalloporphyrins and $\mathbf{C_{60}}$:[9a]

$$\text{ZnP}^{\cdot-} + C_{60} \rightarrow \text{ZnP} + C_{60}^{\cdot-}$$

Interestingly, the rates hardly differ in defiance of a large variation in driving force for the examined metalloporphyrins ($-\Delta G_{ET}° = 0.2$–0.8 eV), a result typical for nearly diffusion-controlled reactions. In the toluene–acetone–propan-2-ol solvent composite (8 : 1 : 1 v/v) k_{diff} amounts to 3.5×10^9 $M^{-1}s^{-1}$. Despite these facts, the low reduction potentials of tin(IV) porphyrins (**SnP**) led to the observation of equilibrium conditions between these two molecules (**SnP** and $\mathbf{C_{60}}$) and their respective one-electron reduced forms ($\mathbf{SnP}^{\cdot-}$ and $\mathbf{C_{60}}^{\cdot-}$). Rate and equilibrium constants have been established by following the decay and formation kinetics, of the $\mathbf{SnP}^{\cdot-}$ and $\mathbf{C_{60}}^{\cdot-}$, respectively, as well as by determination of their relative yields at different $[\mathbf{C_{60}}]/[\mathbf{SnP}]$ concentration ratios. The actual figures are: $k = 3.2 \times 10^9$ $M^{-1}s^{-1}$, $k_{-} = 2.1 \times 10^8$ $M^{-1}s^{-1}$,

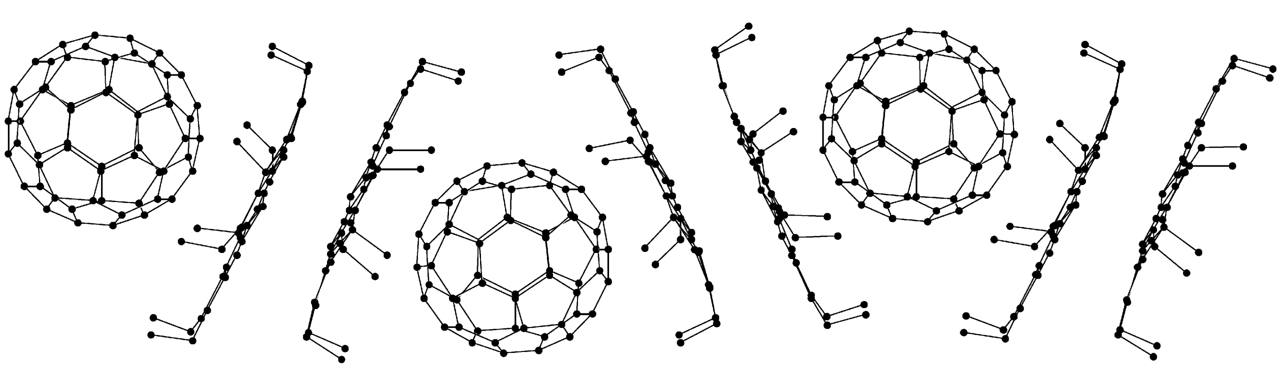

Fig. 1 A view of chains of $\mathbf{C_{60} \cdot 2CoOEP}$.[10a]

and $K = 14 \pm 3$. The equilibrium constant was used to calculate an even smaller λ-value for **$\mathbf{C_{60}}$** in electron transfer of 0.48 eV. The smaller value may be, in part, due to the intrinsic properties of the solvent mixtures (*i.e.*, relative permittivity and refractive index).

$$\mathrm{SnP}^{\bullet -} + \mathrm{C}_{60} \leftrightharpoons \mathrm{SnP} + \mathrm{C}_{60}^{\bullet -}$$

It should be stated that the radiolysis experiments led to just one radical species—either a one-electron reduced **$\mathbf{MP}^{\bullet -}$** or **$\mathbf{C_{60}}^{\bullet -}$**—without, however, producing the corresponding counter radical cation. By contrast, during the course of the photolysis, ion pairs, that is the radical anion and radical cation, are formed. In polar solvents, for instance, an *inter*molecular electron transfer evolves in **ZnP/$\mathbf{C_{60}}$** mixtures from both triplet states, **^{3*}ZnP** (**P** denotes tetraphenyl- and octaethylporphyrin) and **$^{3*}\mathbf{C_{60}}$** to yield **$\mathbf{ZnP}^{\bullet +}/\mathbf{C_{60}}^{\bullet -}$** radical pairs. The exact pathway depends on the excitation wavelength, exciting either **ZnP** or **$\mathbf{C_{60}}$**:[11]

$$^{3*}\mathrm{ZnP} + \mathrm{C}_{60} \rightarrow \mathrm{ZnP}^{\bullet +} + \mathrm{C}_{60}^{\bullet -}$$

$$\mathrm{ZnP} + {}^{3*}\mathrm{C}_{60} \rightarrow \mathrm{ZnP}^{\bullet +} + \mathrm{C}_{60}^{\bullet -}$$

Spectroscopically, the photoproducts are identified with relative ease by characteristic absorption changes in the visible and near-infrared: maxima around 650 nm are clear attributes of the **$\mathbf{ZnP}^{\bullet +}$**, while transient absorbances at 1000 nm resemble the diagnostic marker of the fullerene radical anion, **$\mathbf{C_{60}}^{\bullet -}$**.

The quantum efficiency for electron transfer is higher upon employing the better electron donating octaethylporphyrin in combination with **$\mathbf{C_{60}}$** than the tetraphenylporphyrin analog. Conversely, non-polar media favor *inter*molecular triplet–triplet energy transfer from **^{3*}ZnP** to **$\mathbf{C_{60}}$**:

$$^{3*}\mathrm{ZnP} + \mathrm{C}_{60} \rightarrow \mathrm{ZnP} + {}^{3*}\mathrm{C}_{60}$$

Decisive evidence for such electron transfer processes—*via* the triplet–triplet route—came from FT-EPR experiments,[11*b*,*c*] which give rise to resonance peaks associated with **$\mathbf{C_{60}}^{\bullet -}$** and **$^{3*}\mathbf{C_{60}}$**, corroborating that both energy and electron transfer processes occur between **ZnP** and **$\mathbf{C_{60}}$**. Furthermore, from the analyses of the spin polarization and the time-evolution, it was concluded that the electron spin polarization of **^{3*}ZnP** is transferred to **$^{3*}\mathbf{C_{60}}$**, conserving the spin angular momentum.

5 Stabilization of the charge-separated state—charge-recombination in the inverted region

Considering the experimentally determined λ values of 0.48 and 0.6 eV,[9] which are remarkably small compared to other artificial model acceptors (0.8–1.2 eV), the thermodynamic maximum ($-\Delta G_{\mathrm{ET}}^{\circ} = \lambda$) and, therefore, access to the 'inverted-region' ($-\Delta G_{\mathrm{ET}}^{\circ} > \lambda$) should be reached with relative ease. Now, any reaction that renders strongly exothermic shifts deep into the 'inverted-region', as charge-recombination processes typically are, and its rate is largely slowed-down. An additional benefit of a small λ value is that the 'normal-region' ($-\Delta G_{\mathrm{ET}}^{\circ} > \lambda$) becomes steeper, which is expected to accelerate the charge-separation.

In this regard, a finding by Gust *et al.* is of fundamental importance.[12] In the first example of a C$_{60}$-based system (**1**), in which the two π-electron systems are essentially in van der Waals contact, they found that charge-recombination is significantly slower than charge-separation. This pioneering work evoked the synthesis of a virtually unlimited number of C$_{60}$-based donor–acceptor ensembles integrating a variety of organic electron-donor molecules *via* covalent bonds.[12–16]

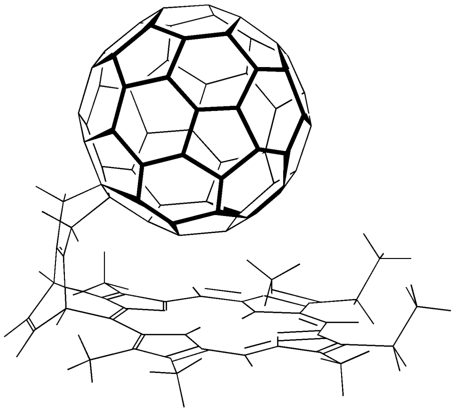

1

A particularly promising set of ensembles turned out to be the choice of **ZnP**, covalently linked, for instance, to several pyrrolidino- or methanofullerene derivatives as artificial reaction centers, in which the complicated natural mechanism can be reduced to its basic elements. An exemplification is given in Fig. 2. Excitation of the **ZnP** portion with visible light, which leads predominantly to the population of its first singlet excited state, **^{1*}ZnP**, is followed by a rapid *intra*molecular electron transfer (k_{CS}) to yield a long-lived charge-separated state in high yields:

$$\mathrm{ZnP\text{-}C_{60}} \xrightarrow{h\nu} {}^{1*}\,\mathrm{ZnP\text{-}C_{60}} \rightarrow \mathrm{ZnP}^{\bullet +}\text{-}\mathrm{C}_{60}^{\bullet -}$$

Importantly, a significant fraction of the photon energy is converted and stored in the form of **$\mathbf{ZnP}^{\bullet +}$–$\mathbf{C_{60}}^{\bullet -}$**. Alternatively, the energetic charge-separated state may evolve from **$^{1*}\mathbf{C_{60}}$** (k_{CS}'). This pathway is, however, of minor importance, since it infers either the very unlikely event of direct **$\mathbf{C_{60}}$** excitation or the competing transfer of singlet excitation energy (k_{EN}).

$$\mathrm{ZnP\text{-}C_{60}} \xrightarrow{h\nu} \mathrm{ZnP\text{-}}{}^{1*}\mathrm{C}_{60} \rightarrow \mathrm{ZnP}^{\bullet +}\text{-}\mathrm{C}_{60}^{\bullet -}$$

$$\mathrm{ZnP\text{-}C_{60}} \xrightarrow{h\nu} {}^{1*}\mathrm{ZnP\text{-}C_{60}} \rightarrow \mathrm{ZnP\text{-}}{}^{1*}\mathrm{C}_{60} \rightarrow \mathrm{ZnP}^{\bullet +}\text{-}\mathrm{C}_{60}^{\bullet -}$$

To exemplify the advantages of incorporating a fullerene, a C$_{60}$-based porphyrin dyad should be compared with a quinone-based analog.[17] Since comparable reduction potentials, donor–acceptor separations and electronic couplings guarantee similar $-\Delta G_{\mathrm{ET}}^{\circ}$'s, any effects must be connected with the different reorganization energies. In fact, accelerated charge-separation (~6 times) and decelerated charge-recombination processes (~25 times), by which the C$_{60}$-based system excels the corresponding quinone dyad, are an impressive proof of the above hypothesis.

Thus, at the beginning of our own photophysical investigation, we anticipated seeing a deceleration of the energy-wasting and undesirable charge-recombination. Recently we accomplished a definite verification of this assumption by demonstrating that charge-recombination, in a series of C$_{60}$-containing donor–acceptor ensembles, occurs indeed in the 'inverted-region'.[18] Here, the selection of **ZnP** showed how crucial is the correct choice of the *intra*molecular separation in light-driven electron transfer reactions, especially to ensure $-\Delta G^{\circ} >> \lambda$. A novel fullerene–porphyrin conjugate with van der Waals contacts (*edge-to-edge* separation (R_{ee}) ~3.0 Å) such as, for example ***trans*-2-ZnP-$\mathbf{C_{60}}$**, reminiscent of the ***trans*-1-ZnP-$\mathbf{C_{60}}$** ensemble (not shown) reported by Diederich *et al.*,[13*h*] provided an exquisite setting for this study. The short separation guaranteed that an *intra*molecular charge-separation succeeds in virtually any solvent and dominates over the competing energy transfer. This is illustrated in Fig. 3, showing the rapid

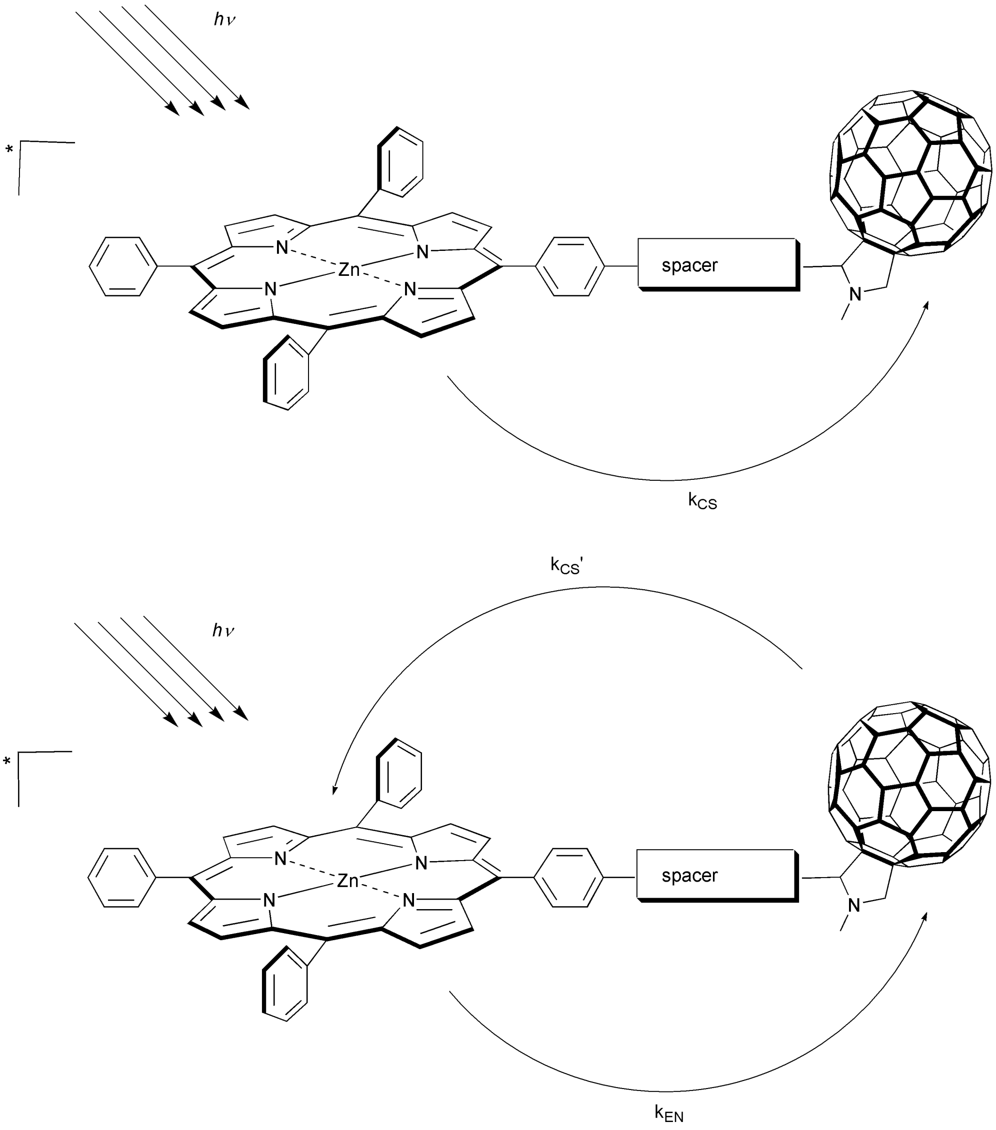

Fig. 2 Schematic illustrations of the charge-separation pathways in **ZnP-C$_{60}$** ensembles, following visible light excitation.

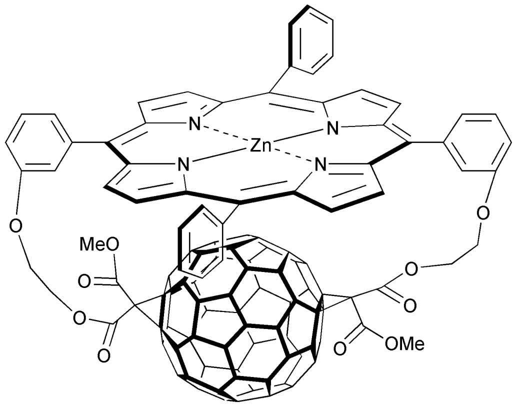

***trans*-2-ZnP-C$_{60}$**

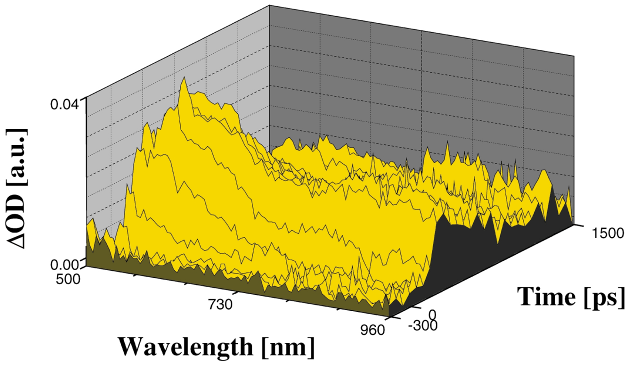

Fig. 3 Differential absorption spectra obtained upon picosecond flash photolysis (532 nm) of ~ 10^{-5} M solutions of ***trans*-2-ZnP-C$_{60}$** in nitrogen saturated toluene with time delays between −300 and 1500 ps, showing the growth and decay of the charge-separated state.

formation and decay of **ZnP**$^{\cdot+}$ between 670–680 nm and **C$_{60}$**$^{\cdot-}$ around 900 nm in toluene, due to charge-separation and charge-recombination processes, respectively. Changing the solvent polarity between non-polar toluene and polar benzonitrile provided the means to alter the free energy changes over a wide range. But, most importantly, a marked acceleration of the charge-recombination rates was seen at smaller $-\Delta G_{CR}°$, namely, at higher relative permittivities, which corroborated nicely our working hypothesis. For instance, the lifetimes varied between 619 ps (toluene) and 38 ps (benzonitrile). Correlating log (k_{ET}) with $-\Delta G_{ET}°$ (*i.e.*, charge-separation and charge-recombination) and fitting of the resulting parabolic dependence yielded an experimental λ value of 0.86 eV. A possible explanation for this somewhat large value (*vide infra*) is that the tight stacking of the two moieties is a responsible force for mutually perturbing the π-systems.

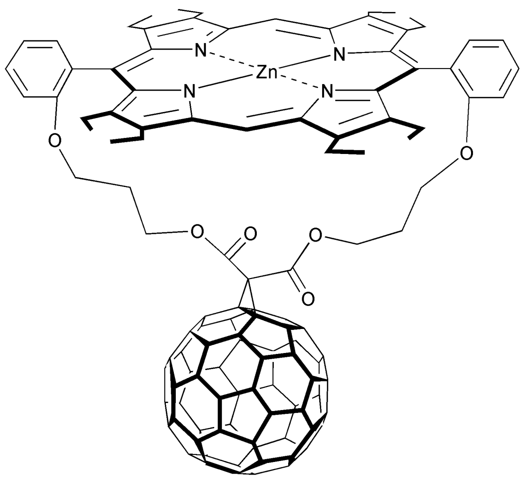

***parachute*-ZnP-C$_{60}$**

An independent and elegant work by Schuster *et al.* manifested that the same outstanding trend holds also in a ***parachute*-ZnP-C$_{60}$**:[19] slower charge-recombination dynamics at larger $-\Delta G_{CR}°$. However, due to the slightly looser stacking, a longer-lived **ZnP$^{\cdot+}$-C$_{60}$**$^{\cdot-}$ radical pair (69 ps in benzonitrile) was seen than in ***trans*-2-ZnP-C$_{60}$**. A recent modeling suggests that the porphyrin bends over to sit in a much closer position, relative to the fullerene, than earlier anticipated. The tendency, that a wider separation retards the charge-recombination, points already to an important direction (*vide infra*).

In a different approach, the charge-recombination rates in ***pyrrole*-ZnP$^{\cdot+}$-C$_{60}$**$^{\cdot-}$ with ***pyrrole*-H$_2$P$^{\cdot+}$-C$_{60}$**$^{\cdot-}$ (**H$_2$P** = free base tetraphenylporphyrin) were identified as a potent means for varying the free energy changes ($-\Delta G_{CR}°$), namely, from 1.38 eV to 1.58 eV without, however, modifying the medium (*i.e.*, benzonitrile).[20] The corresponding lifetimes of 290 ps and 50 ps furnish essentially the same conclusion, *viz.* the dynamics within these radical pairs are consistent with the occurrence of charge-recombination in the 'inverted region' of the Marcus parabola.

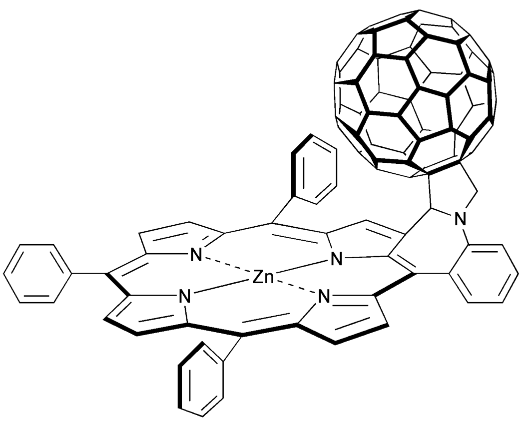

***pyrrole*-ZnP-C$_{60}$**

6 Tuning the coupling, orientation and separation in donor–acceptor dyads

In this review, the discussion shall be limited to some selected examples outlining several unprecedented trends, although an armada of **ZnP-C$_{60}$** arrays has appeared in recent years.[12,13,15–20] The examples were chosen to disclose the most fundamental and most far-reaching impact that fullerene research imposes on our understanding of charge-separation processes. Here the overriding principles can be summarized as gaining control over the (*i*) electronic coupling, (*ii*) geometrical overlap and (*iii*) nature of the intervening spacer in donor–acceptor ensembles. The key objective is to highlight parameters associated with the formation of energetic charge-separated states in synthetic reaction center models.

At this point, reference should be made to the excellent contributions by Imahori and Sakata[15a,d] and Gust, Moore and Moore,[15h,i] in which several key issues were reviewed that are, however, not covered in the present work, such as synthetic aspects.

In general, attachment of the various porphyrin moieties—porphyrin malonates or porphyrin aldehydes—to C$_{60}$ has been achieved by standard reactions in fullerene chemistry, such as cyclopropanation reactions (so called Bingel reaction),[6] 1,3-dipolar cycloaddition of azomethine ylides,[21a] or else [4 + 2] cycloadditions.[21b] These reactions imply relatively simple steps and have afforded a wide variety of fullerene–porphyrin ensembles.[12,13,15–20]

The first class encompasses linear arrays, in which a systematic variation of the spatial distance, separating the donor (**ZnP**) from the acceptor (**C$_{60}$**), to about 11.9 Å (R_{ee}), but preserving the overall free energy changes (*i.e.*, in polar solvents), leads to lifetimes as large as 2.7 microseconds in deoxygenated THF (see Table 1).[22] The reader should be reminded of the picosecond lifetime in the closest **ZnP/C$_{60}$** packing possible (see ***trans*-2-ZnP-C$_{60}$**). Thus, this approach has increased the lifetime of charge-separation by a factor of nearly 7000. All these model systems are structurally well-defined assemblies in which both moieties are held at fixed distances and orientations. The reorganization energies, as far as they were determined, describe an interesting distance dependence: first they drop from 0.86 eV (R_{ee} = 3.0 Å) to ~0.5 eV (R_{ee} = 6.18 Å)[18] before they steadily increase to 0.66 eV (R_{ee} = 11.9 Å).[21] On the other hand, the electronic coupling (V) decreases with distance throughout all the systems from 415 cm^{-1} (R_{ee} = 3.0 Å) to 3.9 cm^{-1} (R_{ee} = 11.9 Å). Therefore, in general, it can be stated that the reorganization energies are indeed smaller than those reported previously for porphyrin–quinone and zinc porphyrin–free base porphyrin linked systems, which typically are in the range between 0.8 eV and 1.2 eV.[23]

Comparing ***trans*-2-ZnP-C$_{60}$** with the topographically different ***equatorial*-ZnP-C$_{60}$**, provided a unique set of models suitable for unraveling effects associated with the geometrical arrangement of donor and acceptor (*i.e.* face-to-face *versus* face-to-edge).[24] The modification of the relative alignment, as it was accomplished synthetically through a different positioning of the two connecting tethers at the fullerene core, alters the π–π interactions. The variance in spatial overlap is reflected in the electronic coupling, which differs by as much as 350 cm^{-1}. Another important result is the change of the charge-separated state lifetime: 4 orders of magnitude difference shifts the lifetime from the lower picosecond (***trans*-2-ZnP-C$_{60}$**) to the microseconds regime (***equatorial*-ZnP-C$_{60}$**; benzonitrile: 1.1 μs). Equally important is to realize the fact that the *face-to-edge* alignment in the ***equatorial*** isomer renders a good access to both cores. This affects crucially the solvation stabilization, ensuring much better interactions with the charge-separated radical pair, compared to the less accessible moieties given by the *face-to-face* geometry in the ***trans*-2** analog, in which, for example, most of the porphyrin surface is covered by the fullerene.

A surprising result comes from a fundamentally different type of linkage, in which flexibility of the spacer unit is being provided by connecting the **ZnP/C$_{60}$** couple with –O-CH$_2$-CH$_2$-O– units of differing composition.[24b] This contrasts with the work on steroid-,[13f] amide-,[22] norbornylogous-linkages,[13b] where the structural rigidity of the spacer is the overriding principle. Furthermore, an altered substitution pattern on the **ZnP**'s phenyl moieties, namely, ***meta-*** *versus* ***para-***, affects the spatial overlap between the two moieties. This notion is further

Table 1 Lifetimes of charge-separated states in various (**ZnP/C$_{60}$**)-based donor–acceptor ensembles at room temperature

Compound	THF	Benzonitrile	DMF	Other solvents
***trans*-2-ZnP-C$_{60}$**	385 ps	38 ps		619 ps[b]
***parachute*-ZnP-C$_{60}$**	99 ps	69 ps	56 ps	
***parachute*-H$_2$P-C$_{60}$**	314 ps	155 ps	107 ps	
***pyrrole*-ZnP-C$_{60}$**		50 ps		
***pyrrole*-H$_2$P-C$_{60}$**		290 ps		
***equatorial*-ZnP-C$_{60}$**	2.6 μs	1.1 μs	0.21 μs	
***meta*-ZnP-C$_{60}$**	215 ns	113 ns	99 ns	
***para*-ZnP-C$_{60}$**	236 ns	149 ns	133 ns	
***norbornylogous*-ZnP-C$_{60}$**		420 ns		
***amide*-ZnP-C$_{60}$**	2.7 μs	0.78 μs	0.57 μs	
ZnP-H$_2$P-C$_{60}$	34 μs	21 μs	20 μs	
Fc-ZnP-C$_{60}$	3.7 μs	7.5 μs	16 μs	
Fc-H$_2$P-C$_{60}$		8.3 μs	19 μs	
Fc-ZnP-H$_2$P-C$_{60}$		0.38 s[a]		
(ZnP)$_3$-ZnP-H$_2$P-C$_{60}$				1.3 ns[c]
ZnP-*pyridine*-C$_{60}$	*inter*molecular	*inter*molecular		
DABCO-ZnP-C$_{60}$				1.98 ns[b]
C$_{60}$-ZnP-DABCO-ZnP-C$_{60}$				2.28 ns[b]
***meta*-ZnP-C$_{60}$-ZnP**				150 ns[d]
***para*-ZnP-C$_{60}$-ZnP**				290 ns[d]
***para*-(DABCO)-ZnP-C$_{60}$-ZnP**				702 ns[d]

[a] Frozen matrix. [b] Toluene. [c] 2-Methyltetrahydrofuran. [d] *o*-Dichlorobenzene.

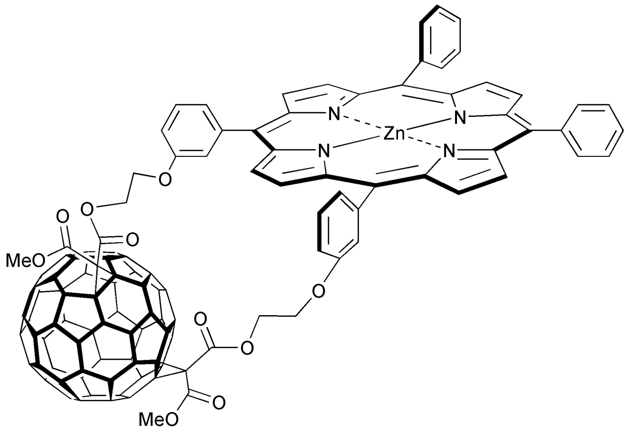

***equatorial*-ZnP-C$_{60}$**

furnished by molecular modeling, which suggests that not only a different R_{ee}, but, most importantly, a deviant overlap governs the ***meta*-** and ***para*-ZnP-C$_{60}$** configuration, as depicted in Fig. 4. Charge-transfer absorption and charge-transfer emission, as meaningful attributes for electronic interactions, indeed corroborate this hypothesis.

The van der Waals stacked dyad (*i.e.*, ***trans*-2-ZnP-C$_{60}$**; 3 Å) and ***amide*-ZnP-C$_{60}$** (R_{ee} = 11.9 Å)[22] emerge as ideal model systems, due to their limited interaction distance. As far as the charge-transfer absorption in these systems is concerned, its intensity drops as a function of separation in virtually any given solvent in the following order: ***trans*-2-ZnP-C$_{60}$** (ε = 1470 M^{-1} cm^{-1}) > ***meta*-ZnP-C$_{60}$** (ε = 740 M^{-1} cm^{-1}) > ***para*-ZnP-C$_{60}$** (ε = 10 M^{-1} cm^{-1}). By contrast, due to the linear positioning of the redox moieties at opposite ends in ***amide*-ZnP-C$_{60}$** no charge-transfer features were seen at all.[22d] Overall, the electronic coupling, which was derived from these spectroscopic assets, reveals a resembling tendency varying from 436 cm^{-1} to 3.9 cm^{-1}.

The energetic separation between charge-transfer absorption and emission assists in determining the reorganization energy in at least non-polar solvents, such as benzene and toluene. Polar solvents, on the other hand, prevent this type of analysis, since non-radiative processes deactivate the charge-transfer state, instead of the emissive transition. The λ-values are unprecedentedly small, at least in comparison with other artificial model systems and are approaching those established for the PRC (~0.2 eV). For example, at room temperature ***meta*-ZnP-C$_{60}$** gives rise to 0.16 eV in toluene. Substantially larger values must, however, be extrapolated for more polar solvents.

In general, all dyads investigated reveal destabilization of the charge-separated state in polar solvents. This trend even holds for ***para*-ZnP-C$_{60}$**, in which the weakest coupling among the series of dyads suggests that the semi-flexible –O-CH$_2$-CH$_2$-O– chain must be the inception for some configurational changes, once photoexcited. Just for comparison, the *meta*-linkage ensures a better, tighter stacking of the **ZnP** onto the fullerene moiety (see Fig. 4). Nevertheless, the charge-recombination dynamics are similar in these two flexibly linked donor–acceptor ensembles, namely, several hundred nanoseconds (***para*-ZnP-C$_{60}$**: 149 ns; ***meta*-ZnP-C$_{60}$**: 113 ns; both in benzonitrile). The small, but notable, changes found in virtually all the investigated solvents, can be correlated with the different donor strength of the *meta- versus para*-substituted **ZnP**. As a consequence of the *para*-isomer's higher oxidation potential, larger free energy changes determine the charge-recombination process, shifting the kinetics deeper into the inverted region. From this we infer that in the charge-separated state the **ZnP$^{\cdot+}$** and **C$_{60}$$^{\cdot-}$** moieties take similar separations relative to each other in both dyads. It cannot be ruled out, however, that the smaller coupling, which prevails in this donor–acceptor ensemble, may have an equal contribution.

One of the major conclusions, as it certainly evolves from all these versatile studies, is that an ideal electron transfer scenario implies charge-separation close to the thermodynamic maximum ($-\Delta G_{CS}° = \lambda$) to minimize the activation barrier. Based on the data known so far $-\Delta G_{CS}°$ ~ 0.6 eV appears to be a good reference point. In addition, $-\Delta G_{CR}°$ should be as large as possible, namely, $>> \lambda$. **ZnP-C$_{60}$** ensembles certainly meet these requirements quite well, which lends important incentives for the strategy of more complex triad and tetrad structures (*vide infra*). A different aspect of this thermodynamic reasoning reaches out to some technological concerns. It permits the possibility to minimize the loss of excited state energy and, thereby, to improve the conversion efficiency of solar energy into electrical and chemical energy.

In principle, similar effects can be summarized for several **H$_2$P-C$_{60}$** ensembles, making use of flexible and rigid spacer units.[13c,f,19,20] An important design consideration implies that the higher oxidation potential of **H$_2$P$^{\cdot+}$/H$_2$P** couple relative to that of **ZnP$^{\cdot+}$/ZnP** of around 200 mV, would allow storing a larger fraction of the excited state energy as chemical potential

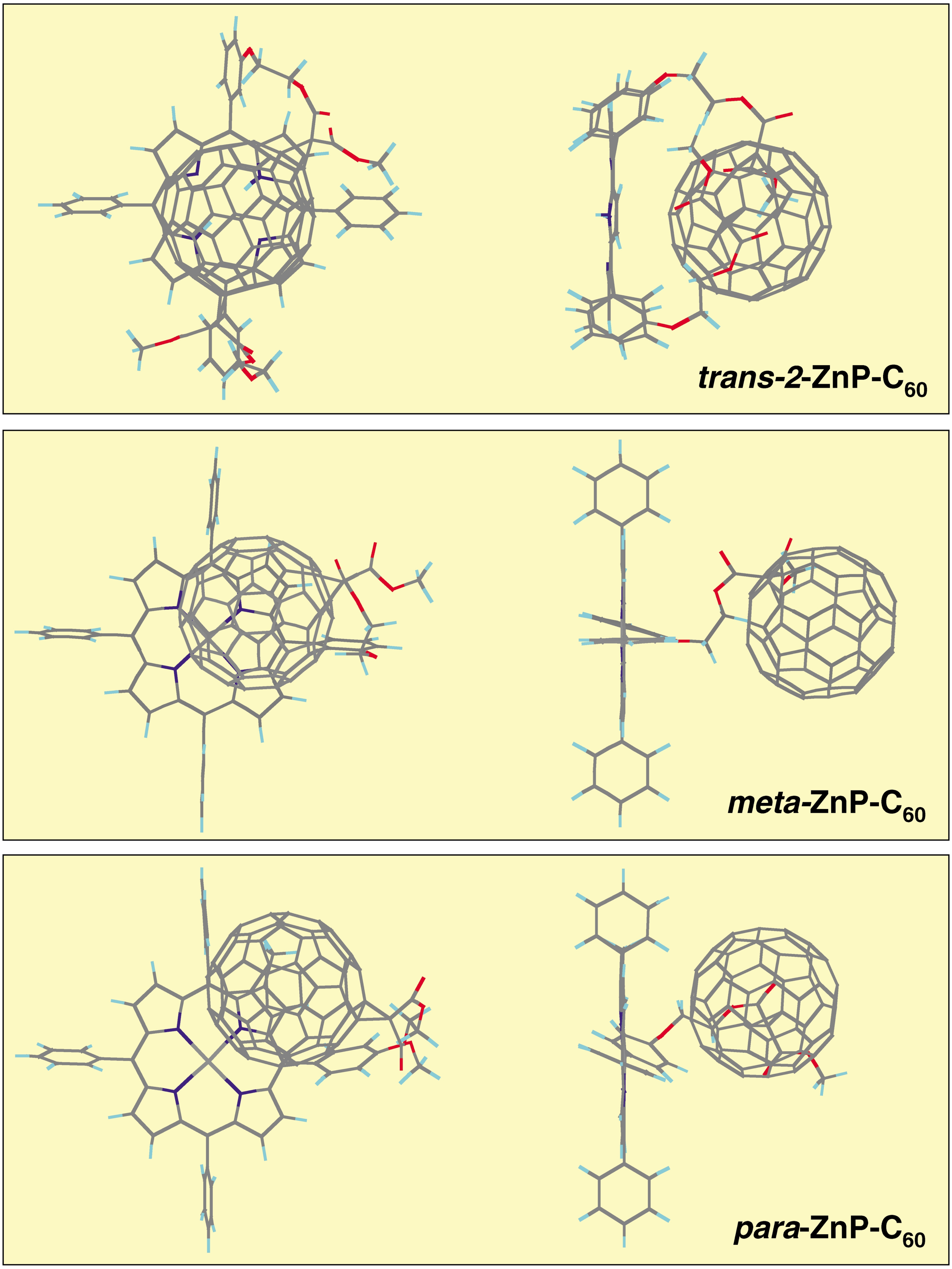

Fig. 4 Top and side views of overlapping fullerene and porphyrin moieties in ***trans*-2-ZnP-C_{60}**, ***meta*-ZnP-C_{60}** and ***para*-ZnP-C_{60}**.

in the charge-separated state. Fig. 5 structures the kinetic schemes for the photoinduced relaxation and deactivation processes in **H_2P-C_{60}** as compared to **ZnP-C_{60}**. From the energetic point of view, slower k_{CS} and k_{CR} are logical consequences that stem from the energy gap variation in **H_2P-C_{60}** *versus* **ZnP-C_{60}** ensembles.

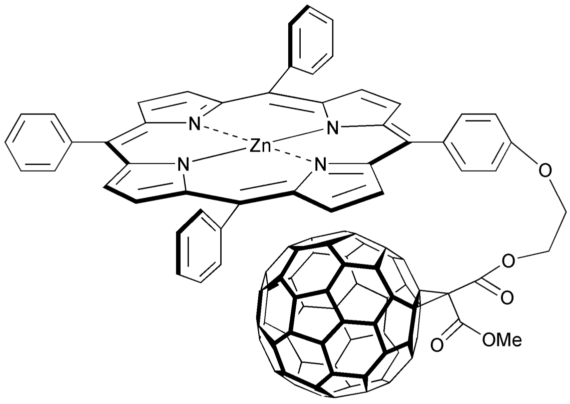

para-ZnP-C_{60}

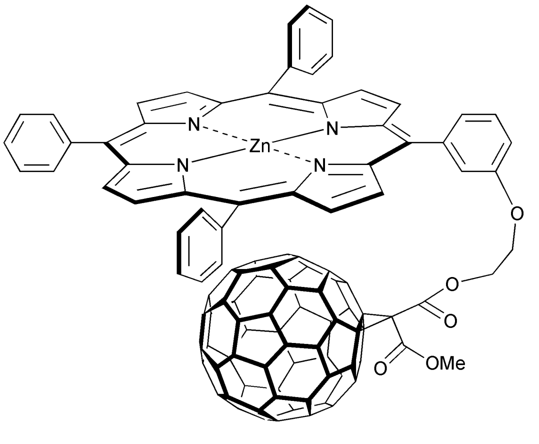

meta-ZnP-C_{60}

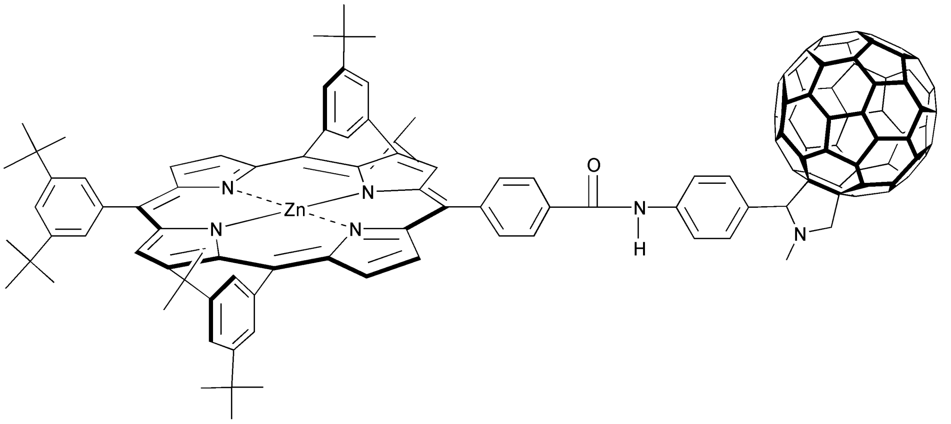

amide-ZnP-C_{60}

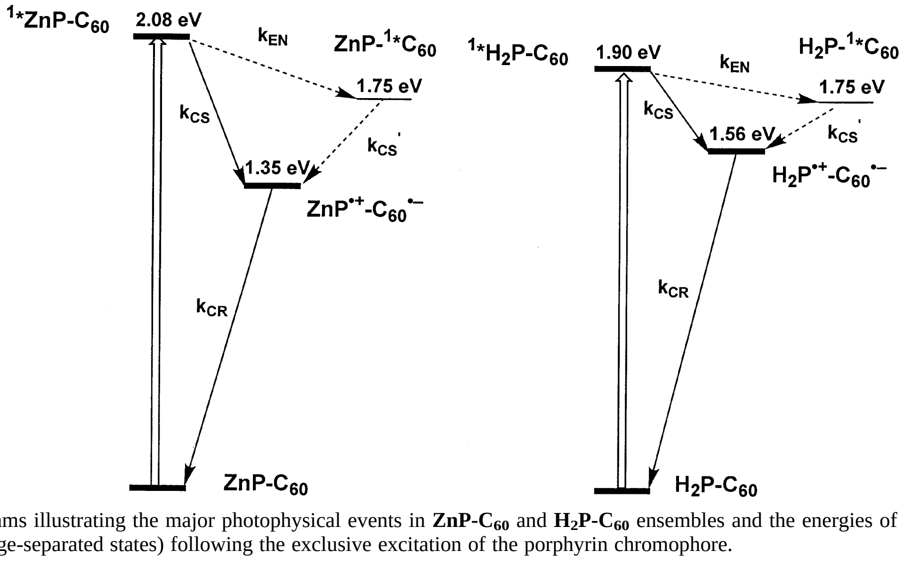

Fig. 5 Energetic diagrams illustrating the major photophysical events in **ZnP-C_{60}** and **H_2P-C_{60}** ensembles and the energies of the associated states (*i.e.*, excited states and charge-separated states) following the exclusive excitation of the porphyrin chromophore.

Interestingly, substitution of the electron acceptor unit **C_{60}** by **C_{70}**, which is a slightly better electron acceptor, leads to a two-fold expedition of the charge-separation dynamics (k_{CS}).[13e]

7 Linear donor–acceptor ensembles—triads and tetrads

Encouraged by these remarkable results, several linear triads (R_{ee} = 30.3 Å) and tetrads (R_{ee} = 48.9 Å) were built around the **ZnP/C_{60}** couple as artificial reaction centers. We probed in collaboration with Imahori *et al.* the lifetime of the charge-separated state *via* systematically extending the donor–acceptor composition.[22,25,26] Despite the multifaceted difficulties, connected with the design of rigidly spaced ensembles containing more than just a single donor–acceptor couple, it is imperative to realize that a long-distance and long-lived charge-separated state can only be attained in a series of short-range, fast and efficient electron transfer systems unless wire-like spacer units are employed. A specific challenge involves attaining a fine-tuned and directed redox gradient along donor–acceptor linked arrays.

The first promising results stem from a set of molecular triads in which a fullerene moiety is linked either to an array of two porphyrins (*i.e.*, **ZnP** and **H_2P**; **ZnP-H_2P**)[22a,c] or to a **Fc-ZnP** fragment.[25b,d] In the **ZnP-H$_2$P-C$_{60}$** triad, the **ZnP** moiety performs as an antenna molecule, transferring its singlet excited state energy to the lower lying **H$_2$P**. In polar benzonitrile, this energy transfer is followed by a sequential electron transfer yielding **ZnP-H$_2$P$^{\cdot+}$-C$_{60}$$^{\cdot-}$** ($\tau$ = 77 ns) and subsequently **ZnP$^{\cdot+}$-H$_2$P-C$_{60}$$^{\cdot-}$** ($\tau$ = 21 μs). Considering the overall efficiency of 40% for (*i*) funneling light from the antenna chromophore (*i.e.*, **ZnP**) to the **H$_2$P** chromophore, (*ii*) charge-injection into the fullerene core and (*iii*) charge-shift, this artificial reaction center reproduces the natural system very well.[19a]

The lifetimes of **ZnP$^{\cdot+}$-H$_2$P-C$_{60}$$^{\cdot-}$** in different media correlate well with the polarity: 34 μs (THF), 21 μs (benzonitrile), 20 μs (DMF). Since the driving force of charge-recombination ($-\Delta G_{\mathrm{CR}}°$) decreases even in **ZnP-H$_2$P-C$_{60}$** with increasing solvent polarity, the observed trend suggests that the associated rate constants are in the 'inverted region' of the Marcus curve.[22c]

The function of the **Fc-ZnP-C$_{60}$** and **Fc-H$_2$P-C$_{60}$** systems, on the other hand, is a lot simpler and limited to two consecutive electron transfers yielding the **Fc$^+$-ZnP-C$_{60}$$^{\cdot-}$** and **Fc$^+$-H$_2$P-C$_{60}$$^{\cdot-}$** in nearly 82 and 25% yield, respectively.[22c,25b] In oxygen-free benzonitrile, the final charge-separated state decays, however, considerably faster to the singlet ground state than does the **ZnP$^{\cdot+}$-H$_2$P-C$_{60}$$^{\cdot-}$** ($4.8 \times 10^4$ s^{-1}). The actual rate constants are 1.3×10^5 s^{-1} (**Fc$^+$-ZnP-C$_{60}$$^{\cdot-}$**) and 1.2×10^5 s^{-1} (**Fc$^+$-H$_2$P-C$_{60}$$^{\cdot-}$**). Taking into account the similarity in molecular structure and separation (R_{ee} = 30.3 Å) the different thermodynamics must be responsible for this intrinsic behavior. In fact, variation of the $-\Delta G_{\mathrm{CR}}°$ (*i.e.*, comparing THF and DMF) led to a surprising discovery: the dynamics within the **Fc$^+$/C$_{60}$$^{\cdot-}$** couples are in the 'normal region' of the Marcus curve, that is, $-\Delta G < \lambda$.[22c]

In general, electronic coupling (V) and reorganization energy (λ) further corroborate the trend seen in the **ZnP-C$_{60}$** dyads: diminished couplings and increased reorganization energies accompany the larger separation (R_{ee} = 30.3 Å). Precisely, the following values were derived for the **ZnP-H$_2$P-C$_{60}$/Fc-H$_2$P-C$_{60}$** ensembles (λ = 1.09 eV; V = 0.019 cm^{-1}) from Fig. 6.

Replacement of **Fc** by a carotenoid secondary electron donor (**Car**) in **Car-ZnP-C$_{60}$** and **Car-H$_2$P-C$_{60}$**, led to a fundamentally different picture.[27] Now, the carotenoid triplet excited state moves energetically between those of the final radical pair and of the ground state. Thus, the product of the charge-recombination is predominantly the **^{3*}Car-H$_2$P-C$_{60}$**, and the dynamics must, although located still in the 'inverted region', occur with $-\Delta G_{\mathrm{CR}}° \sim \lambda$, that is, near the top of the Marcus parabola. For example, in polar solvents $-\Delta G_{\mathrm{CR}}°$ is 0.6 eV. Most interestingly, lowering the temperature to 77 K increases the lifetime of **Car$^{\cdot+}$-H$_2$P-C$_{60}$$^{\cdot-}$** from 60 ns to 325 ns in 2-methyltetrahydrofuran.

Successful mimicry of the primary events in photosynthesis using **ZnP-H$_2$P-C$_{60}$** and **Fc-ZnP-C$_{60}$** encouraged us to combine these two systems into an integrated single system, **Fc-ZnP-H$_2$P-C$_{60}$**.[26] Indeed, the lifetime of the spatially-separated (R_{ee} = 48.9 Å) radical pair, the product of a sequence of energy and multistep electron transfer reactions, reaches well beyond milliseconds (0.38 s), into a time domain which has never been accomplished so far in an artificial photosynthetic reaction center. As reference points 340 μs and 12.7 ms are reported for synthetic systems in room temperature solutions and at 77 K, respectively, which further document the conceptional breakthrough in our work. The lifetime is also comparable, for example, to the lifetimes (~1 s^{-1}) of the bacteriochlorophyll dimer radical cation ((Bchl)$_2$$^{\cdot+}$)–secondary quinone radical anion (Q$_B$$^{\cdot-}$) ion pair in the bacteria PRC. The relatively low quantum yields (0.17–0.24) can be rationalized by the competition of the various charge-shift reactions, transferring the charge from **Fc-ZnP-H$_2$P$^{\cdot+}$-C$_{60}$$^{\cdot-}$** to **Fc$^+$-ZnP-H$_2$P-C$_{60}$$^{\cdot-}$** *versus* the intrinsic decays of the reactive intermediates. It should also be

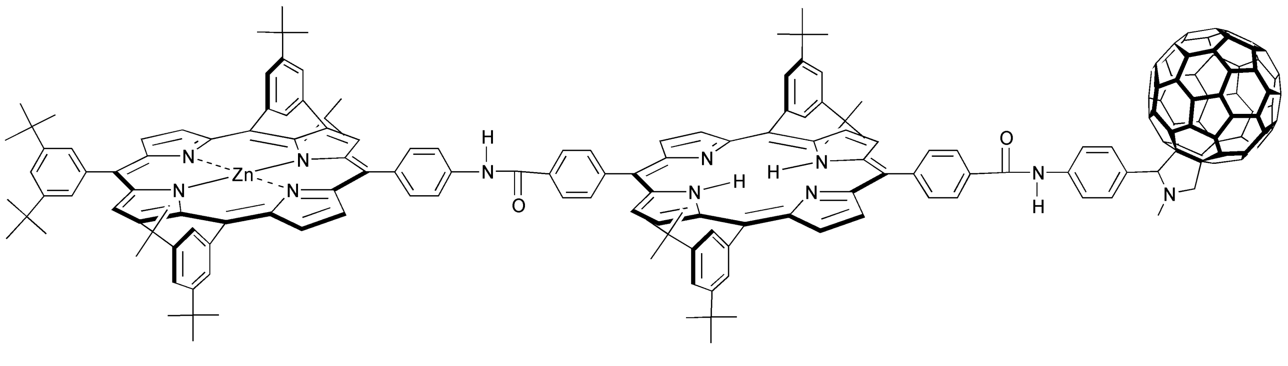

ZnP-H$_2$P-C$_{60}$

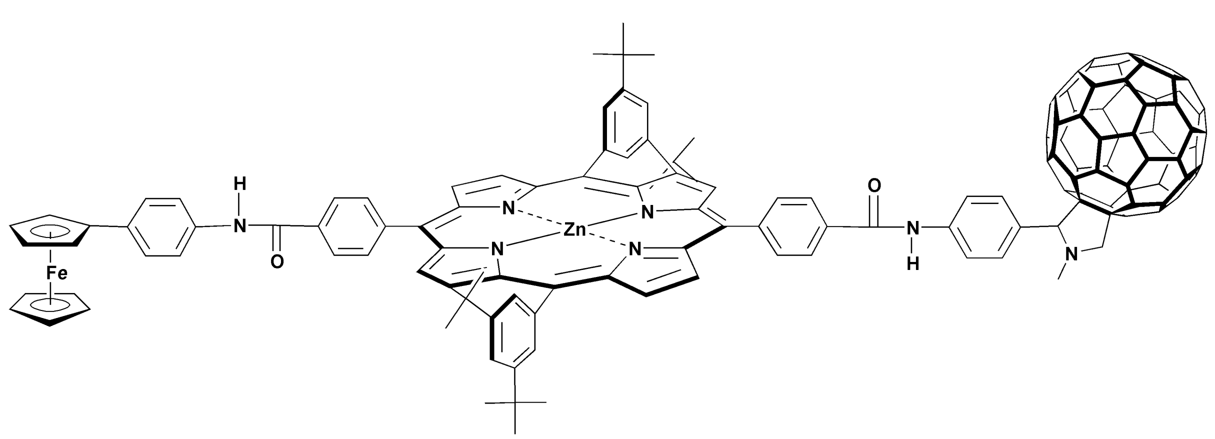

Fc-ZnP-C$_{60}$

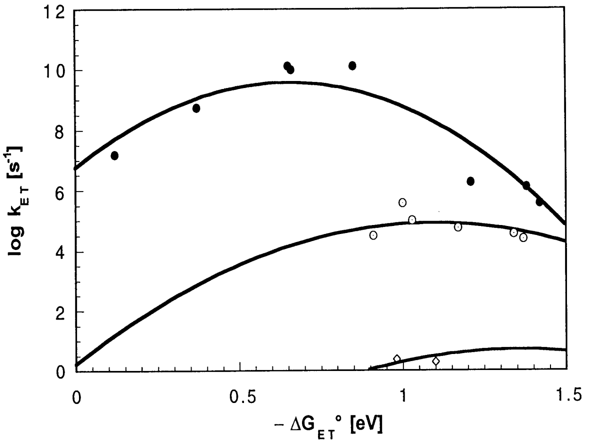

Fig. 6 Driving force ($-\Delta G_{ET}°$) dependence of intramolecular charge-separation and charge-recombination rate constants in ***amide*-ZnP-C_{60}** dyad (top curve), **ZnP-H_2P-C_{60}/Fc-H_2P-C_{60}** triads (center curve) and **Fc-ZnP-H_2P-C_{60}** tetrad (bottom curve).

emphasized that such an extremely long lifetime of the tetrad system has been well correlated with the charge-separated lifetimes of two homologous series of porphyrin–fullerene dyad and triad systems. In essence the longer lifetimes, smaller coupling elements (**Fc-ZnP-H_2P-C_{60}**: 1.7×10^{-4} cm^{-1}) and larger reorganization energies (**Fc-ZnP-H_2P-C_{60}**: 1.32 eV) are clear characteristics of these systems (*vide supra*).

In **Fc-ZnP-H_2P-C_{60}**, one of the limiting parameters is certainly the charge-injection from **$^{1*}H_2P$** into the fullerene acceptor to yield **Fc-ZnP-$H_2P^{\cdot+}$-$C_{60}^{\cdot-}$**. To facilitate this crucial step—by avoiding this bottle-neck—the first charge-separation step should be probed in a **Fc-ZnP-ZnP-C_{60}** tetrad. In general, **ZnP** has a lower oxidation potential, thus providing more thermodynamic driving force, and therefore potentially larger rate constants and quantum yields for the crucial conversion of the **Fc-ZnP-^{1*}ZnP-C_{60}** intermediate to the **Fc-ZnP-$ZnP^{\cdot+}$-$C_{60}^{\cdot-}$** species.

Unquestionably, the most striking and far reaching observation is that charge-recombination in all these **$ZnP^{\cdot+}$/$C_{60}^{\cdot-}$** couples (*i.e.*, dyads and triads) is located in the 'inverted region' of the Marcus parabola, regardless of linkage, distance and orientation. By contrast, lowering the driving force *via* replacing the **ZnP** with the better electron acceptor ferrocene (**Fc**), while keeping all other parameters (*i.e.*, distance, acceptor, solvent, temperature, *etc.*) constant, shifts the dynamics into the normal region. This variation is of great advantage in determining parameters such as electronic coupling (*V*), reorganization energy (λ) and damping factor (β) with high accuracy. They all have key features for material design considerations with the objective being to prolong the lifetime of the energetic charge-separated state, while, simultaneously, optimizing the efficiency of charge separation.

8 Branched donor–acceptor ensembles—hexad

Quite remarkably, a sophisticated **(ZnP)$_3$-ZnP-H_2P-C_{60}** hexad, comprised of a **(ZnP)$_3$-ZnP** model antenna system linked to a

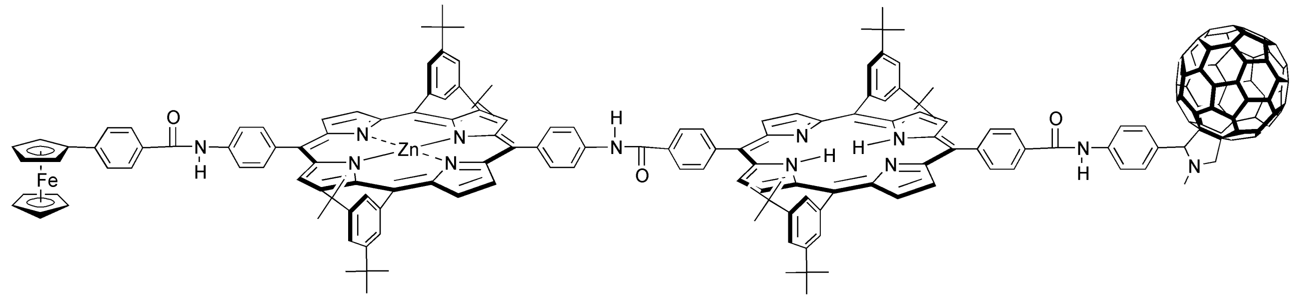

Fc-ZnP-H_2P-C_{60}

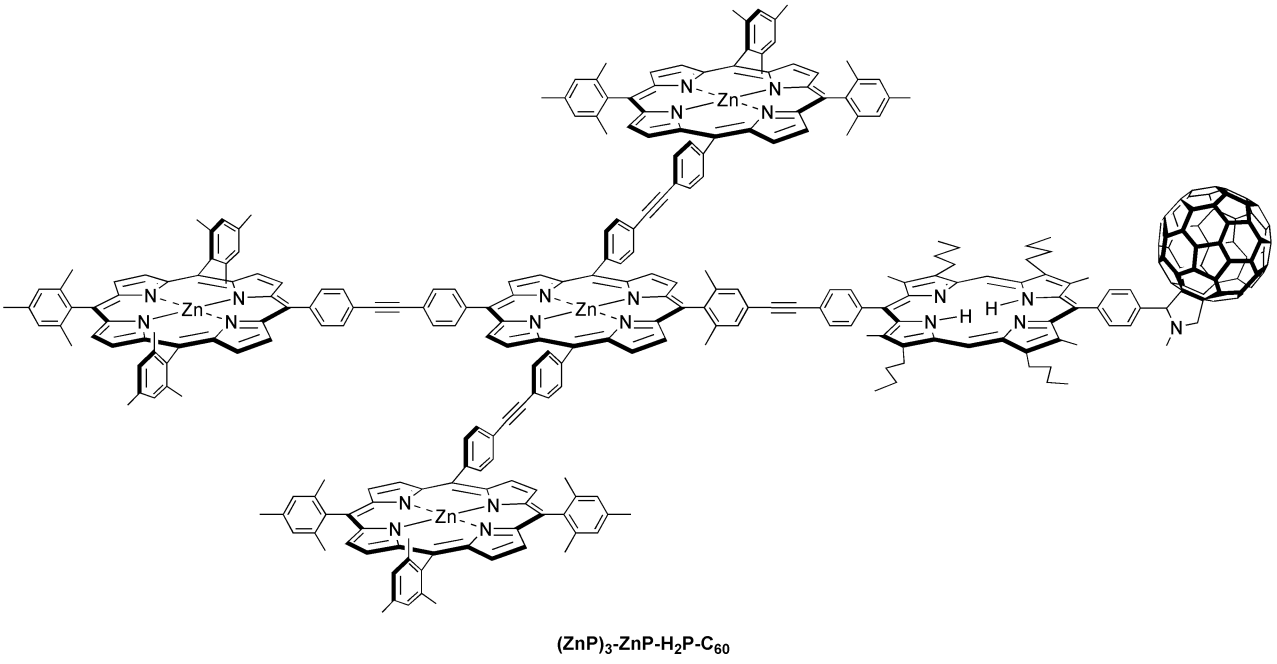

(ZnP)$_3$-ZnP-H_2P-C_{60}

H_2P-C_{60} reaction center, has been shown to reveal indeed a cascade of efficient light-driven energy and electron transfer processes.[28] Specifically, the antenna portion reveals rapid transduction (~50 ps) of the singlet excited energy from the peripheral **$(ZnP)_3$** to the central **ZnP**, which itself transfers the excitation energy further to the **H_2P** chromophore of the reaction center with a rate of 4.2×10^9 s^{-1}. In the final part of the sequence, the resulting **$(ZnP)_3$-ZnP-$^{1*}H_2P$-C_{60}** is the precursor state for an electron transfer process to the electron accepting **C_{60}**. The net result of this complex chain of events is a 1.3 ns long lived charge-separated **$(ZnP)_3$-ZnP-$H_2P^{\cdot+}$-$C_{60}^{\cdot-}$** radical pair, formed in 70% yield. In conclusion this hexad mimics the basic function of both natural photosynthetic antenna systems and reaction center complexes.

9 Self-assembled donor–acceptor ensembles

A better control over the separation, angular relationships, electronic coupling and composition in donor–acceptor assemblies at a molecular level is a formidable task—especially in artificial antenna and reaction centers—to control the rates and yields of energy and electron transfer reactions and to eliminate

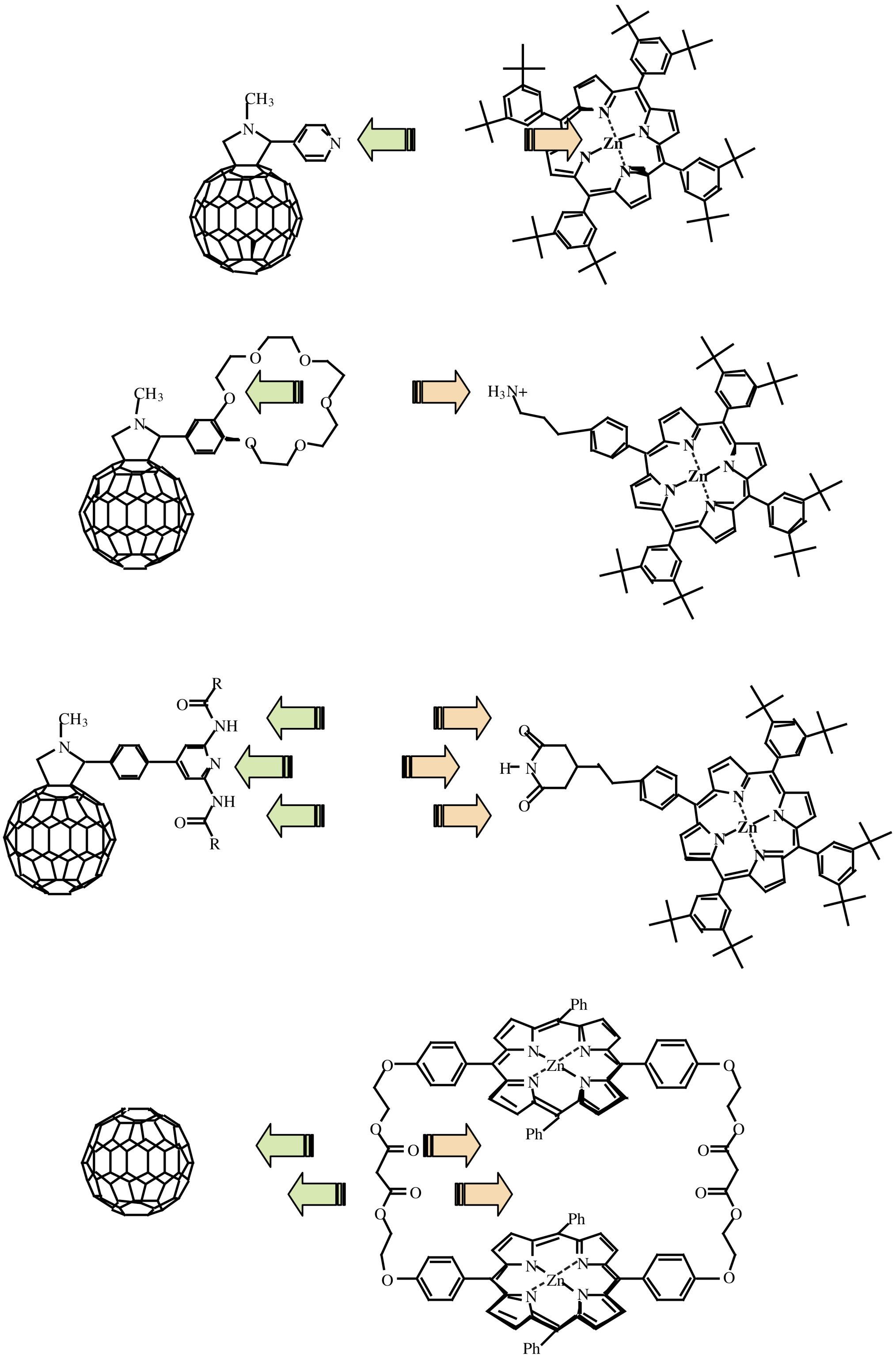

Fig. 7 Self-organizing motifs.

the energy wasting charge-recombination. Meaningful incentives can be borrowed from the organization-principle in the bacterial photosynthetic reaction center: the different light- and redox-active components are embedded *via* non-covalent interactions into a protein matrix. In principle, biomimetic methodologies, such as hydrogen-bonding, donor–acceptor complexation, electrostatic interactions and π–π stacking, guarantee the control over modulating the composition and, simultaneously, achieving well-defined and rigid architectures, with high directionality and selectivity. Thus, self-assembled donor–acceptor ensembles are a viable alternative to supermolecular polyads (*e.g.*, triads, tetrads, *etc.*), involving covalent links between the components, for increasing the rate, yield and lifetime of the charge-separated state. Typical examples of self-organizing ensembles are illustrated in Fig. 7.

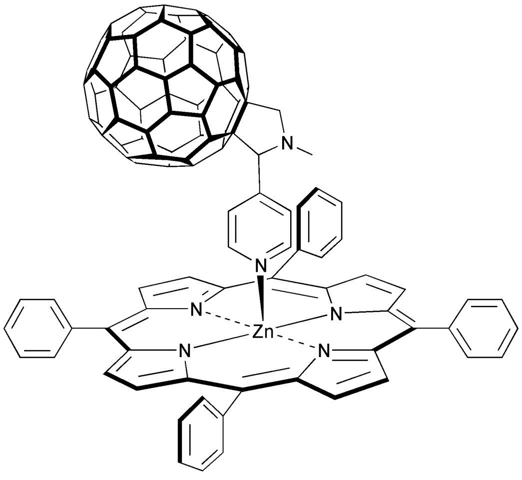

ZnP-*pyridine*-C$_{60}$

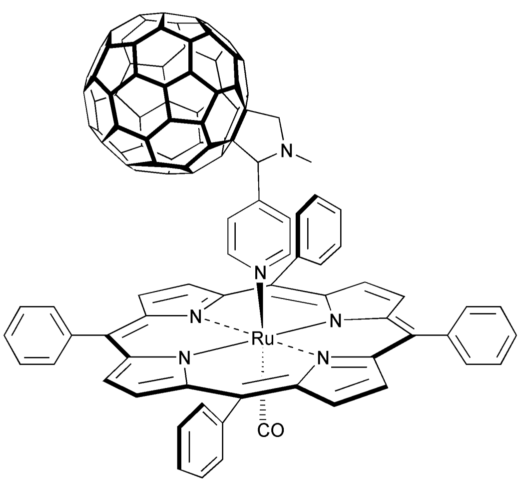

RuP-*pyridine*-C$_{60}$

A first demonstration was presented in the form of a **ZnP-*pyridine*-C$_{60}$** complex. In this, the reversible coordination of a pyridine functionalized fullerene ligand (***pyridine*-C$_{60}$**) to the square-planar zinc center constitutes a labile but, nevertheless, measurable (K ~ 5000 M^{-1}) binding motif, explored by three different research teams simultaneously.[29–31] The ground state features of **ZnP** in the visible (Q-bands) were employed as sensitive aids to monitor the progression of the **ZnP-*pyridine*-C$_{60}$** complexation: red-shifted transitions and the observance of clear isosbestic points. In a chain of events (Fig. 8)—triggered by light—the excited donor activates a rapidly occurring electron transfer to the electron accepting **C$_{60}$** within the **ZnP-*pyridine*-C$_{60}$** complex.[29] The weak equilibrium between dissociation and association of the 'metal–pyridine' bond facilitates then, in the final step of the sequence, the crucial break-up of the radical pair, before the competing charge-recombination starts to become a restriction. In **ZnP-*pyridine*-C$_{60}$** the free radical ions (**ZnP$^{\cdot+}$/C$_{60}$$^{\cdot-}$**) live for tens of microseconds in THF and benzonitrile, and any processes, as they may take place, are exclusively governed by an *inter*molecular diffusion. By contrast, in covalently linked donor–acceptor dyads fast charge-recombination prevails, limiting the lifetime of the radical pair to a few nanoseconds (*vide supra*).

$$\text{ZnP} + \textit{pyridine}\text{-C}_{60} \leftrightharpoons \text{ZnP-}\textit{pyridine}\text{-C}_{60}$$

$$\text{RuP} + \textit{pyridine}\text{-C}_{60} \rightarrow \text{RuP-}\textit{pyridine}\text{-C}_{60}$$

In this regard it appeared attractive to us that complexation of ***pyridine*-C$_{60}$** to a ruthenium tetraphenylporphyrin (**RuP**) produces the quite stable **RuP-*pyridine*-C$_{60}$** complex.[29] Here the overriding principle is that utilization of the strong π-back-bonding strengthens the 'metal–pyridine' bond relative to that found in the **ZnP-*pyridine*-C$_{60}$** analog, in which the bonding is limited to a weak σ-character. As a consequence, the *intra*-molecular charge-separated **RuP$^{\cdot+}$-*pyridine*-C$_{60}$$^{\cdot-}$**, as observed

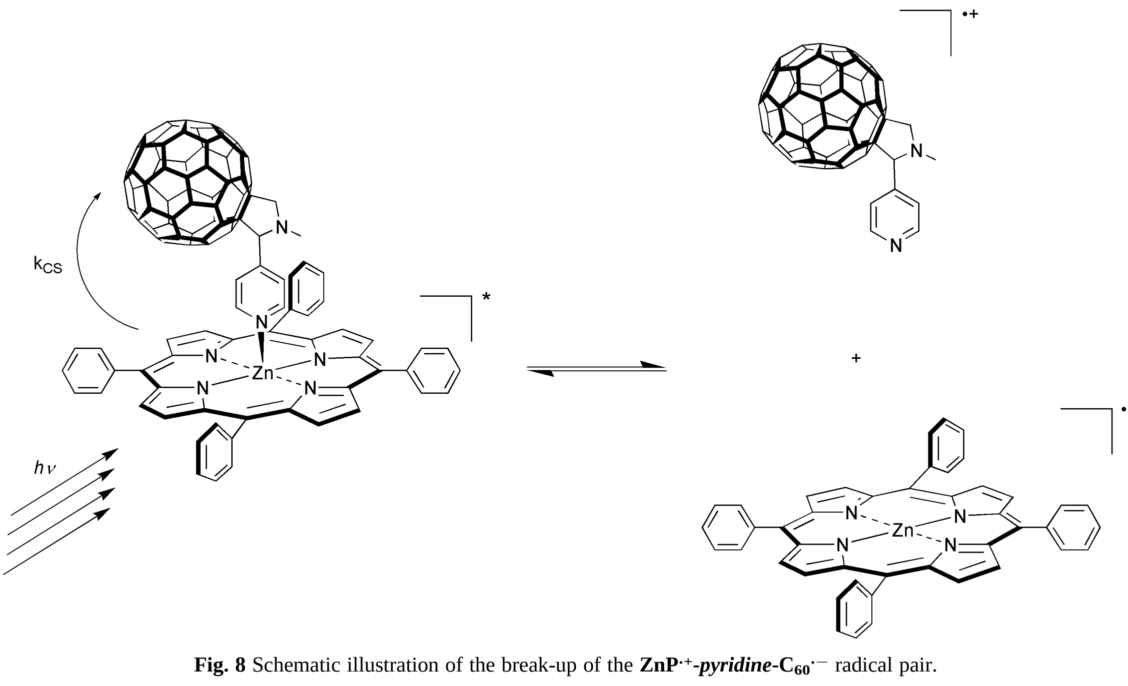

Fig. 8 Schematic illustration of the break-up of the **ZnP$^{\cdot+}$-*pyridine*-C$_{60}$$^{\cdot-}$** radical pair.

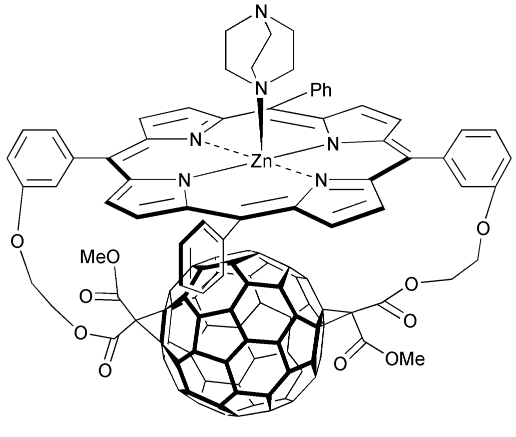

DABCO-ZnP-C$_{60}$

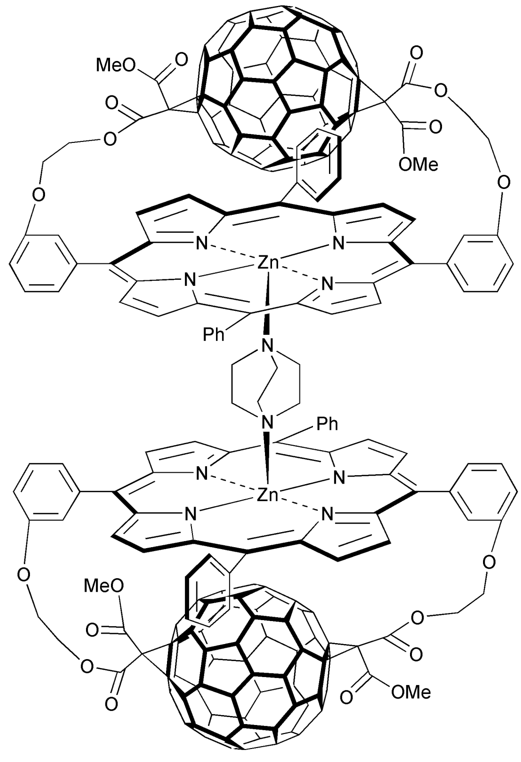

C$_{60}$-ZnP-DABCO-ZnP-C$_{60}$

in polar solvents, recombines rapidly on the picosecond time scale (< 4000 ps), since the diffusional splitting of the radical pair is largely suppressed.

With the objective to devise linear architectures of higher complexity, that is, triads, tetrads and pentads (*vide infra*), several **ZnP/C$_{60}$** containing ensembles were subjected to complexation assays with **di**aza**bi**cyclo**o**ctane (**DABCO**).[32] The bidentate **DABCO** ligand exhibits a number of appealing features: it forms not only square pyramidal 1 : 1- or 2 : 1-complexes with, for example, **ZnP**, but is also a good electron donor. A prerequisite for their successful construction restricts the use to non-coordinating solvents. Suitable polar media, on the other hand, set up a competition between **DABCO** and solvent complexation and lead subsequently to dissociation into the free components. Importantly, charge-recombination kinetics in the primary building block (*i.e.*, ***trans*-2-ZnP-C$_{60}$**, *etc.*)[18] of these complexes reveal that the large $-\Delta G_{\mathrm{CR}}°$ values in toluene are extremely helpful to stabilize the **ZnP$^{\cdot+}$-C$_{60}$$^{\cdot-}$** radical pair. Considering these facts in concert, it is clear that among the many unique fullerene features the small reorganization energy guarantees appreciable affects in these photoactive architectures, especially in light of retarding charge-recombination.

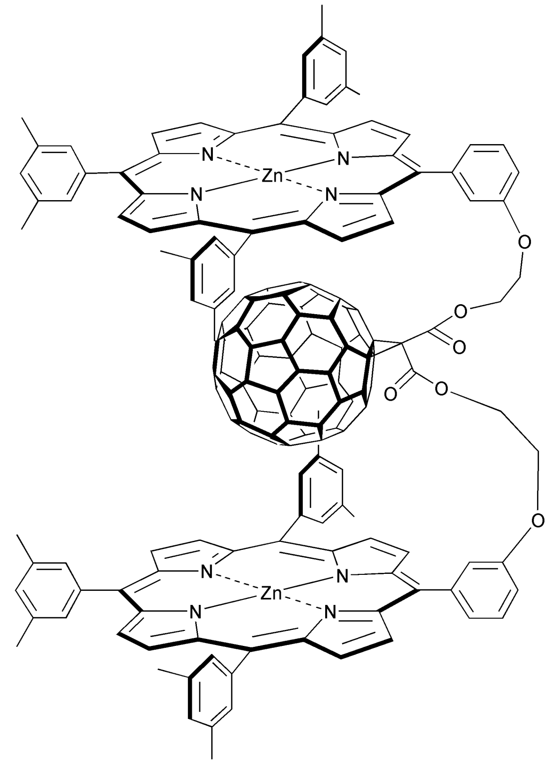

***meta*-ZnP-C$_{60}$-ZnP**

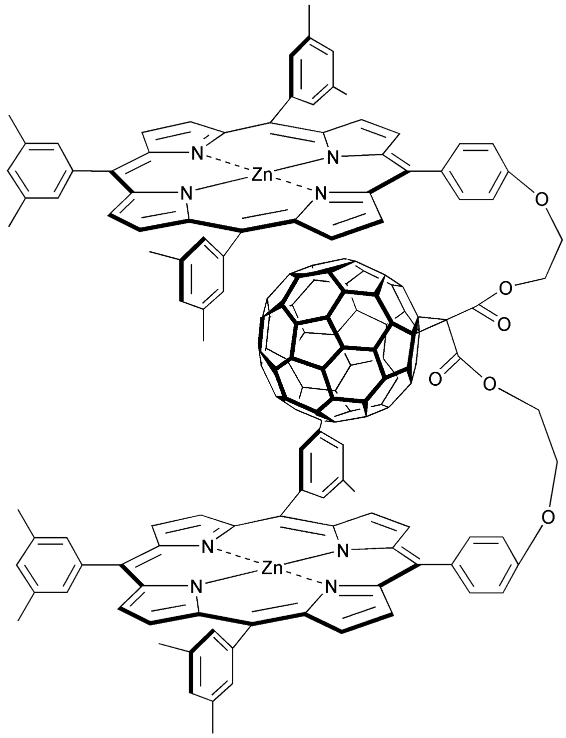

***para*-ZnP-C$_{60}$-ZnP**

Depending on the relative concentrations, namely, that of **DABCO** and ***trans*-2-ZnP-C$_{60}$**, the precursor dyad was consecutively transformed into the **DABCO-ZnP-C$_{60}$** triad and the **C$_{60}$-ZnP-DABCO-ZnP-C$_{60}$** pentad. In these new ensembles, similar electron transfer rates (~ 10^{11} s^{-1}) convert the photoexcited chromophore state into the different charge-separated states. The lifetimes of the latter vary markedly with the ensemble constitution, indicating that subsequent charge-shift reactions, indeed, take place, prior to the decay to the singlet ground state. For example, a significant improvement is seen upon going from ***trans*-2-ZnP$^{\cdot+}$-C$_{60}$$^{\cdot-}$** (toluene: τ = 619 ps)

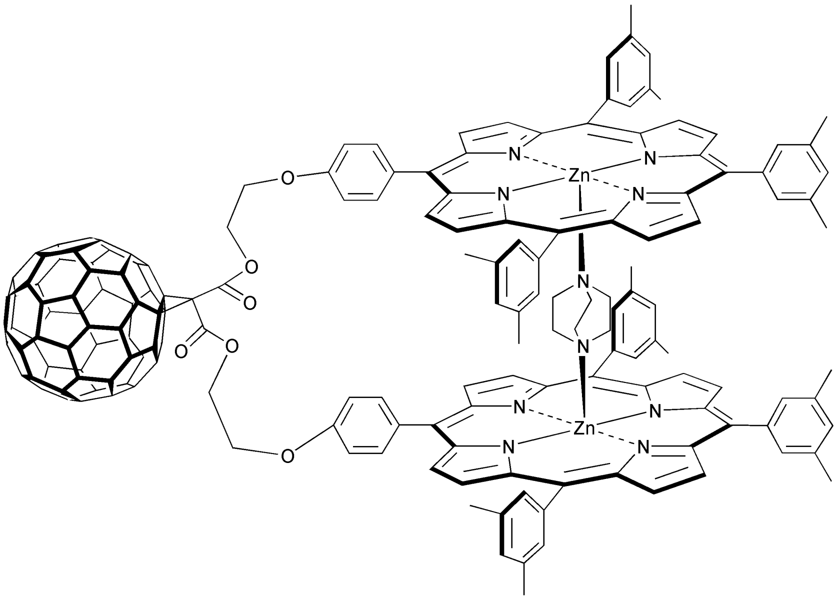

***para*-(DABCO)-ZnP-C$_{60}$-ZnP**

and **DABCO$^{\cdot+}$-ZnP-C$_{60}^{\cdot-}$** (toluene: τ = 1980 ps) to **C$_{60}$-ZnP-DABCO$^{\cdot+}$-ZnP-C$_{60}^{\cdot-}$** (toluene: τ = 2280 ps). The close energy of the **DABCO-ZnP$^{\cdot+}$-C$_{60}^{\cdot-}$** and **DABCO$^{\cdot+}$-ZnP-C$_{60}^{\cdot-}$** states implies that the positive charge may be distributed over both moieties, instead of being located exclusively on **DABCO**. In summary, the simple addition of extra components, which self-assemble to the precursor in a controlled manner, is an effective mode to gain control over the charge-recombination rates.

A different example involves a simplistic but powerful means to regulate donor–acceptor separations and orientations. More precisely, rigid, confined model ensembles are self-assembled, starting from a flexible **ZnP-C$_{60}$-ZnP** system and **DABCO**.[33] Similar to the simpler dyad ensembles (*i.e.*, ***meta*-ZnP-C$_{60}$** and ***para*-ZnP-C$_{60}$**) a photoinduced electron transfer evolving from the **ZnP** singlet excited state to the electron accepting fullerene governs the photophysics of the ***meta*-ZnP-C$_{60}$-ZnP** and the more electron-rich ***para*-ZnP-C$_{60}$-ZnP**. The resulting **ZnP$^{\cdot+}$-C$_{60}^{\cdot-}$-ZnP** states decayed on a time scale of a few hundred nanoseconds to regenerate the ground state. For example, in *o*-dichlorobenzene the actual values are 150 ns and 290 ns in the ***meta*-ZnP-C$_{60}$-ZnP** and ***para*-ZnP-C$_{60}$-ZnP** isomers, respectively.

Addition of **DABCO** to toluene or *o*-dichlorobenzene solutions of ***meta*-ZnP-C$_{60}$-ZnP** or ***para*-ZnP-C$_{60}$-ZnP** evoked a strong reactivation of the **^{1*}ZnP** fluorescence (factor of ~ 3). A similar impact was concluded from the transient absorption measurements, monitoring the decay and grow-in kinetics of **^{1*}ZnP** and **ZnP$^{\cdot+}$/C$_{60}^{\cdot-}$** features, respectively. The sum of these effects evokes a model that infers the successful complexation of **DABCO** to the vacant sites of the two **ZnP** (*i.e.*, dz^2-orbitals) to expand the donor–acceptor separation considerably (*i.e.*, triad *versus* tetrad). In polar media (*i.e.*, *o*-dichlorobenzene) these readily available and stable ensembles are subject to a rapid *intra*molecular electron transfer to yield a long-lived radical pair with lifetimes close to a microsecond (~ 700 ns). Again, the simple addition of a suitable component leads to a nearly five-fold improvement of the radical pair stability, besides an overall higher quantum yield of formation (Φ). Conversely, in a non-polar medium (*i.e.*, toluene) energy transfer replaces electron transfer in deactivating the photo-excited chromophore, **^{1*}ZnP**, forming, in the final instance, the fullerene triplet excited state.

In retrospect, the reversible coordination of **DABCO** to **ZnP-C$_{60}$-ZnP** creates a simple photoswitch, in which either an electron or energy transfer pathway deactivates the photoexcited **ZnP**. Larger **DABCO** concentrations, however, lead to the precipitation of poorly soluble oligomeric materials. It is interesting to note that the lifetime of the radical pair in these not well-defined structures gives rise to a further improvement (7.5 μs): a sufficiently fast separation of charges along the longitudinal axis is probably responsible for this consequence.

An appealing feature of the zinc-coordination is that the bond to an axially bond **DABCO** in a five-coordinated, square pyramidal Zn-complex is particularly labile. To prove that addition of a complexing agent will ultimately result in the destruction of the rigid donor–acceptor ensemble we added, for example, THF to an *o*-dichlorobenzene solution and probed the **ZnP** fluorescence. Indeed, a decrease in emission suggests the successful decomplexation, while removal of the volatile THF component led again to the reactivation of the emission. Unequivocally, this confirms the reversible transformation and, thereby, topological control over the donor–acceptor separation and orientation. Important for the performance of these fluorescing probes is the fact that, after probing this activation–deactivation cycle up to ten times, no notable deviation from the reversibility was found.

10 Future developments

Recent advances with respect to utilizing molecular recognition in the form of macrocyclic receptor molecules open new opportunities to control the dynamics of *intra*molecular events in the form of a supramolecularly assembled **ZnP** (*i.e.*, porphyrin box, porphyrin cube and porphyrin tweezers)–**C$_{60}$** system.[34] This constitutes certainly an elegant approach to assemble discrete van der Waals complexes bearing a close resemblance to natural photosynthesis.

Interesting developments will also include the use of T_h-hexadducts, in which the role of fullerene is to serve as the structure determining tecton.[35] The highly symmetric T_h-core facilitates loading of the fullerene core, for instance, with a shell of up to six electron donor/chromophore moieties, which renders these systems particularly appealing for photoconversion processes. Important features will include constructing larger light harvesting arrays and storing larger fractions of photonic energy in the charge-separated state.

Organic based photovoltaics, in which the knowledge gained during our more fundamentally oriented studies is used to advance the more technological issues, are expected to play an important role.[36]

11 Acknowledgements

This work was supported by the Office of Basic Energy Sciences of the U.S. Department of Energy. This is document NDRL-4338 from the Notre Dame Radiation Laboratory. I am deeply indebted to Professors Fukuzumi, Hirsch, Imahori, Maggini, Martin, Prato and Sakata for their productive collaborations and numerous stimulating discussions. This paper is dedicated to the memory of Ralf O. Guldi (1934-2001).

12 References

1 *The Photosynthetic Reaction Center*, ed. J. Deisenhofer and J. R. Norris, Academic Press, New York, 1993.
2 *Electron Transfer in Chemistry Vol. I–V*, ed. V. Balzani, Wiley-VCH, Weinheim, 2001.
3 *The Porphyrin Handbook*, ed. K. M. Kadish, K. M. Smith and R. Guilard, Academic Press, New York, 1999.
4 R. F. Curl, *Angew. Chem., Int. Ed. Engl.*, 1997, **36**, 1566.
5 L. Echegoyen and L. E. Echegoyen, *Acc. Chem. Res.*, 1998, **31**, 593.
6 *Fullerenes and Related Structures*, ed. A. Hirsch, *Top. Curr. Chem.*, Vol. 199, Springer, Berlin, 1999.
7 R. A. Marcus, *Angew. Chem., Int. Ed. Engl.*, 1993, **32**, 1111.
8 (*a*) S. Fukuzumi, I. Nakanishi, T. Suenobu and K. M. Kadish, *J. Am. Chem. Soc.*, 1999, **121**, 3468; (*b*) S. Larsson, A. Klimkans, L. Rodriguez-Monge and G. Duskesas, *J. Mol. Struct.*, 1998, **425**, 155.
9 (*a*) D. M. Guldi, P. Neta and K.-D. Asmus, *J. Phys. Chem.*, 1994, **98**, 4617; (*b*) D. M. Guldi and K.-D. Asmus, *J. Am. Chem. Soc.*, 1997, **119**, 5744.
10 Leading references: (*a*) M. M. Olmstead, D. A. Costa, K. Maitra, B. C. Noll, S. L. Phillips, P. M. Van Calcar and A. L. Balch, *J. Am. Chem. Soc.*, 1999, **121**, 7090; (*b*) P. D. W. Boyd, M. C. Hodgson, C. E. F. Rickard, A. G. Oliver, L. Chaker, P. J. Brothers, R. D. Bolskar, F. S. Tham and C. A. Reed, *J. Am. Chem. Soc.*, 1999, **121**, 10487.
11 (*a*) M. E. El-Khouly, M. Fujitsuka and O. Ito, *J. Porphyrins Phthalocyanines*, 2000, **4**, 591; (*b*) J. Fujisawa, Y. Ohba and S. Yamauchi, *Chem. Phys. Lett.*, 1998, **282**, 181; (*c*) D. M. Martino and H. van Willigen, *J. Phys. Chem. A*, 2000, **104**, 10701.
12 P. A. Liddell, J. P. Sumida, A. N. MacPherson, L. Noss, G. R. Seely, K. N. Clark, A. L. Moore, T. A. Moore and D. Gust, *Photochem. Photobiol.*, 1994, **60**, 537.
13 Fullerene–porphyrin donor–acceptor dyads: (*a*) H. Imahori, K. Hagiwara, M. Aoki, T. Akiyama, S. Taniguchi, T. Okada, M. Shirakawa and Y. Sakata, *J. Am. Chem. Soc.*, 1996, **118**, 11771; (*b*) T. D. M. Bell, T. A. Smith, K. P. Ghiggino, M. G. Ranasinghe, M. J. Shephard and M. N. Paddon-Row, *Chem. Phys. Lett.*, 1997, **268**, 223; (*c*) P. S. Baran, R. R. Monaco, A. U. Khan, D. I. Schuster and S. R. Wilson, *J. Am. Chem. Soc.*, 1997, **119**, 8363; (*d*) S. Higashida, H. Imahori, T. Kaneda and Y. Sakata, *Chem. Lett.*, 1998, 605; (*e*) K. Tamaki, H. Imahori, Y. Nishimura, I. Yamazaki, A. Shimomura, T. Okada and Y. Sakata, *Chem. Lett.*, 1999, 227; (*f*) R. Fong, D. I. Schuster and S. R. Wilson, *Org. Lett.*, 1999, **1**, 729; (*g*) M. Wedel and F. P. Montforts, *Tetrahedron Lett.*, 1999, **40**, 7071; (*h*) N. Armaroli, G. Marconi, L. Echegoyen, J.-P. Bourgeois and F. Diederich, *Chem. Eur. J.*, 2000, **6**, 1629; (*i*) S. MacMahon, R. Fong II, P. S. Baran, I. Safonov, S. R. Wilson and D. I. Schuster, *J. Org. Chem.*, 2001, **66**, 5449.
14 Leading references for structural porphyrin analogs and references cited therein: (*a*) N. V. Tkachenko, L. Rantala, A. Y. Tauber, J. Helaja, P. H. Hynninen and H. Lemmetyinen, *J. Am. Chem. Soc.*, 1999, **121**, 9378; (*b*) F. P. Montforts and O. Kutzki, *Angew. Chem., Int. Ed.*, 2000, **39**, 599.
15 For recent reviews on fullerene containing donor–acceptor ensembles and fullerene anions see (*a*) H. Imahori and Y. Sakata, *Adv. Mater.*, 1997, **9**, 537; (*b*) M. Prato, *J. Mater. Chem.*, 1997, **7**, 1097; (*c*) N. Martin, L. Sanchez, B. Illescas and I. Perez, *Chem. Rev.*, 1998, **98**, 2527; (*d*) H. Imahori and Y. Sakata, *Eur. J. Org. Chem.*, 1999, 2445; (*e*) D. M. Guldi, *Chem. Commun.*, 2000, 321; (*f*) D. M. Guldi and M. Prato, *Acc. Chem. Res.*, 2000, **33**, 695; (*g*) C. A. Reed and R. D. Bolskar, *Chem. Rev.*, 2000, **100**, 1075; (*h*) D. Gust, T. A. Moore and A. L. Moore, *J. Photochem. Photobiol. B*, 2000, **58**, 63; (*i*) D. Gust, T. A. Moore and A. L. Moore, *Acc. Chem. Res.*, 2001, **34**, 40.
16 Multiple fullerenes linked to a single porphyrin: (*a*) J.-F. Nierengarten, C. Schall and J.-F. Nicoud, *Angew. Chem., Int. Ed.*, 1998, **37**, 1934; (*b*) J.-F. Nierengarten, L. Oswald and J.-F. Nicoud, *Chem. Commun.*, 1998, 1545; (*c*) A. Rieder and B. Kräutler, *J. Am. Chem. Soc.*, 2000, **122**, 9050.
17 H. Imahori, K. Hagiwara, T. Akiyama, M. Aoki, S. Taniguchi, T. Okada, M. Shirakawa and Y. Sakata, *Chem. Phys. Lett.*, 1996, **263**, 545.
18 (*a*) E. Dietel, A. Hirsch, E. Eichhorn, A. Rieker, S. Hackbarth and B. Röder, *Chem. Commun.*, 1998, 1981; (*b*) D. M. Guldi, C. Luo, M. Prato, E. Dietel and A. Hirsch, *Chem. Commun.*, 2000, 373.
19 (*a*) P. Cheng, S. R. Wilson and D. I. Schuster, *Chem. Commun.*, 1999, 89; (*b*) D. I. Schuster, P. Cheng, S. R. Wilson, V. Prokhorenko, M. Katterle, A. R. Holzwarth, S. E. Braslavsky, G. Klihm, R. M. Williams and C. P. Luo, *J. Am. Chem. Soc.*, 1999, **121**, 11599; (*c*) D. I. Schuster, *Carbon*, 2000, **38**, 1607.
20 (*a*) T. Drovetskaya, C. A. Reed and P. D. W. Boyd, *Tetrahedron Lett.*, 1995, **36**, 7971; (*b*) D. Kuciauskas, S. Lin, G. R. Seely, A. L. Moore, T. A. Moore, D. Gust, T. Drovetskaya, C. A. Reed and P. D. W. Boyd, *J. Phys. Chem.*, 1996, **100**, 15926; (*c*) D. Gust, T. A. Moore and A. L. Moore, *Res. Chem. Intermed.*, 1997, **23**, 621.
21 (*a*) M. Prato and M. Maggini, *Acc. Chem. Res.*, 1998, **31**, 519; (*b*) *Lecture Notes on Fullerenes Chemistry*, ed. R. Taylor, Imperial College Press, London, 1999.
22 (*a*) C. Luo, D. M. Guldi, H. Imahori, K. Tamaki and Y. Sakata, *J. Am. Chem. Soc.*, 2000, **122**, 6535; (*b*) H. Imahori, M. E. El-Khouly, M. Fujitsuka, O. Ito, Y. Sakata and S. Fukuzumi, *J. Phys. Chem. A*, 2001, **105**, 325; (*c*) H. Imahori, K. Tamaki, D. M. Guldi, C. Luo, M. Fujitsuka, O. Ito, Y. Sakata and S. Fukuzumi, *J. Am. Chem. Soc.*, 2001, **123**, 2607; (*d*) H. Imahori, N. V. Tkachenko, V. Vehmanen, K. Tamaki, H. Lemmetyinen, Y. Sakata and S. Fukuzumi, *J. Phys. Chem. A*, 2001, **105**, 1750.
23 Leading references and references cited therein: (*a*) A. Harriman, V. Heitz and J.-P. Sauvage, *J. Phys. Chem.*, 1993, **97**, 5940; (*b*) H. Heitele, F. Pöllinger, T. Häberle, M. E. Michel-Beyerle and H. A. Staab, *J. Phys. Chem.*, 1994, **98**, 7402; (*c*) A. Osuka, G. Noya, S. Taniguchi, T. Okada, Y. Nishimura, I. Yamazaki and N. Mataga, *Chem. Eur. J.*, 2000, **6**, 33.
24 (*a*) D. M. Guldi, C. Luo, M. Prato, A. Troisi, F. Zerbetto, M. Scheloske, E. Dietel, W. Bauer and A. Hirsch, *J. Am. Chem. Soc.*, 2001, **123**, 9166; (*b*) D. M. Guldi, C. Luo, M. Prato, A. Troisi, F. Zerbetto, M. Scheloske, E. Dietel, W. Bauer and A. Hirsch, submitted.
25 (*a*) K. Tamaki, H. Imahori, Y. Nishimura, I. Yamazaki and Y. Sakata, *Chem. Commun.*, 1999, 625; (*b*) M. Fujitsuka, O. Ito, H. Imahori, K. Yamada, H. Yamada and Y. Sakata, *Chem. Lett.*, 1999, 721; (*c*) S. Fukuzumi, H. Imahori, M. E. El-Khouly, M. Fujitsuka, O. Ito and D. M. Guldi, *J. Am. Chem. Soc.*, 2001, **123**, 2571.
26 H. Imahori, D. M. Guldi, K. Tamaki, Y. Yoshida, C. Luo, Y. Sakata and S. Fukuzumi, *J. Am. Chem. Soc.*, 2001, **123**, 6617.
27 (*a*) P. A. Liddell, D. Kuciauskas, J. P. Sumida, B. Nash, D. Nguyen, A. L. Moore, T. A. Moore and D. Gust, *J. Am. Chem. Soc.*, 1997, **119**, 1400; (*b*) D. Carbonera, M. Di Valentin, C. Corvaja, G. Agostini, G. Giacometti, P. A. Liddell, D. Kuciauskas, A. L. Moore, T. A. Moore and D. Gust, *J. Am. Chem. Soc.*, 1998, **120**, 4398; (*c*) J. L. Bahr, D. Kuciauskas, P. A. Liddell, A. L. Moore, T. A. Moore and D. Gust, *Photochem. Photobiol.*, 2000, **72**, 598.
28 D. Kuciauskas, P. A. Liddell, S. Lin, T. E. Johnson, S. J. Weghorn, J. S. Lindsey, A. L. Moore, T. A. Moore and D. Gust, *J. Am. Chem. Soc.*, 1999, **121**, 8604.
29 T. Da Ros, M. Prato, D. M. Guldi, M. Ruzzi and L. Pasimeni, *Chem. Eur. J.*, 2001, **7**, 816.
30 (*a*) F. D'Souza, G. R. Deviprasad, M. S. Rahman and J.-P. Choi, *Inorg. Chem.*, 1999, **38**, 2157; (*b*) F. D'Souza, G. R. Deviprasad, M. E. El-Khouly, M. Fujitsuka and O. Ito, *J. Am. Chem. Soc.*, 2001, **123**, 5277.
31 N. Armaroli, F. Diederich, L. Echegoyen, T. Habicher, L. Flamigni, G. Marconi and J.-F. Nierengarten, *New J. Chem.*, 1999, 77.
32 D. M. Guldi, C. Luo, T. Da Ros, M. Prato, E. Dietel and A. Hirsch, *Chem. Commun.*, 2000, 375.
33 D. M. Guldi, C. Luo, A. Swartz, M. Scheloske and A. Hirsch, *Chem. Commun.*, 2001, 1066.
34 (*a*) K. Tashiro, T. Aida, J.-Y. Zheng, K. Kinbara, K. Saigo, S. Sakamoto and K. Yamaguchi, *J. Am. Chem. Soc.*, 1999, **121**, 9477; (*b*) D. Sun, F. S. Tham, C. A. Reed, L. Chaker, M. Burgess and P. D. W. Boyd, *J. Am. Chem. Soc.*, 2000, **122**, 10704.
35 (*a*) E. Dietel, A. Hirsch, J. Zhou and A. Rieker, *J. Chem. Soc., Perkin Trans. 2*, 1998, 1357; (*b*) X. Camps, E. Dietel, A. Hirsch, S. Pyo, L. Echegoyen, S. Hackbarth and B. Röder, *Chem. Eur. J.*, 1999, **5**, 2362.
36 N. S. Sariciftci, L. Smilowitz, A. J. Heeger and F. Wudl, *Science*, 1992, **258**, 1474.